Kristján Jónasson
Sven Þ. Sigurðsson
Þorsteinn Arnalds

Estimation of avalanche risk

CONTENTS

ABSTRACT

A new operational quantitative procedure for estimation of snow avalanche risk in residential areas, measured as annual probability of being killed, is described. In its present form it is tailored to high hills with some avalanche history, and it is based on a data set of 196 Icelandic avalanches in 81 paths. It makes use of the notions of transferring avalanches between slopes by a physical model (presently a PCM model), and a path independent measure of runout distance, so-called runout index, associated with a specific standard path. Detailed data on the fatalities caused by the avalanches on Súðavík and Flateyri in northwestern Iceland in 1995 is presented and used to derive an empirical relationship between avalanche speed and survival rate, a further ingredient in the method. Two examples of the application of the procedure are presented. It is argued that an acceptable annual death rate due to avalanches is $0.3 \cdot 10^{-4}$ for living houses. A noteworthy preliminary result is that this corresponds to a return period in the range from 3000 to 8000 years.

1   INTRODUCTION

This report explains a hazard zoning method that was first developed at the Science Institute, University of Iceland in 1995-1996 and has been used and further developed at the Icelandic Meteorological Office since mid-year 1996 when two of the authors (KJ and ÞA) moved from the University to there. The work was initiated in reaction to an avalanche falling on the NW Iceland town Súðavík on January 16, 1995, killing 14 people. Most of the houses hit were in an area marked "safe" on the official avalanche hazard map. Work on the zoning method escalated when an avalanche fell on the neighbouring town Flateyri on October 26, 1995, killing 20 people. All were in the "safe" area.

The method is for assessment of avalanche risk in residential areas. The key aspects of the approach are:

- To *measure the avalanche hazard* by calculating the probability of being killed in an avalanche if one lives or works at the place under consideration for a given length of time. We do not deal with economic risk, as the avalanche risk to human life is dominant in Iceland and probably in most other countries.

- To relate the *probability of surviving* an avalanche inside a house at a given site directly to the speed of the avalanche. This relation is based on data from the 1995 avalanches in Súðavík and Flateyri. These avalanches damaged 32 houses where 93 people were staying and, as stated above, 34 of these people were killed.

- To split the estimate of the probability that an avalanche will reach a given site into two separate parts: i) the estimate of the *frequency* at which an avalanche will run beyond a specific reference point above the site, and ii) the estimate of the *distribution of runout distances* of avalanches that exceed the reference point. The latter estimate clearly requires more data, which are obtained by transferring recorded avalanche runout distances from many avalanche paths. The former estimate can be based on more local records.

- To transfer runout distances between paths using *physical models*. In particular this allows direct estimates of the speed at which an avalanche would hit a house located in its path.

- To introduce a slope independent measuring scale for runout distance, so-called *runout indices*, that are based on runout distances transferred to a specified standard path. These allow data from different slopes to be dealt with in a unified manner and facilitate the estimate of the runout distance distribution.

Thus a central assumption is that there exists a scale of runout distances, at least for avalanches typical of those in the underlying data set, so that the distribution of runout distances according to this scale, beyond a given reference distance, is independent of the location of the slope, the shape of the slope, and the frequency of avalanches.

The method is best suited to calculating the risk due to avalanches under hillsides that have *some history of avalanches*. It may also be used for setting an upper limit on the risk when there are no recorded avalanches. Moreover, the current method is tailored to *high hills*, firstly because the avalanches of Súðavík and Flateyri both came from fairly high hills, and secondly because the distribution of runout distances is estimated with high hills in mind. Data from the Súðavík and Flateyri accidents were used to estimate the probability of survival (in both cases the fall height was about 600 m). We have been unwilling to use the method for lower hills than about 350 m.

Estimation of risk due to natural and man-made hazards has been given substantial research attention in recent decades. Some of the hazards that have been considered are earthquakes, meteors (e.g. Chapman and Morrison 1994), nuclear accidents, and aeroplane crashes on towns (e.g. Evans et al. 1997). Until now little work has been done on the direct estimation of avalanche risk to human life. The focus has been on the estimation/calculation of the probable maximum runout distance in a given length of time, but the relation of these estimates to probable loss of human life has been somewhat unclear. Of this nature are the Swiss hazard zoning procedure (see Salm et al. 1990), the runout ratio method of McClung and his co-workers (e.g. McClung et al. 1989) and the alpha-beta model developed at the Norwegian Geotechnical Institute (e.g. Bakkehøi et al. 1983). The latter two methods may be regarded as ways of *transferring* avalanches between paths, which is an important ingredient to the current work. They differ from the transfer methods of our approach in that they are based on topographical considerations rather than physical models. The Swiss procedure, on the other hand, makes use of similar physical models as our approach, but they are used to relate possible snow-depth in starting zones to runout distance.

Recently two interesting dissertations on avalanche risk have been written by Christopher Keylock (1996) and Christian Wilhelm (1997). A paper based on Keylock's dissertation has also been written (Keylock et al. 1998). Keylock gives a procedure for estimating avalanche risk based on McClung's runout-ratio method. Runout distance data of 195 long Icelandic avalanches are used, together with data from two avalanche paths in Canada both with a large number of recorded avalanches, all relatively short. Using Gumbel statistics the distribution of runout distances and the risk of death at a particular place are estimated. While making use of similar data as in our work, Keylock's work was carried out independently and differs in many aspects. Wilhelm's main focus is economic risk, but risk to life is also considered. His work is not based directly on the distribution of runout distances and the associated dependence of death probability on runout distance. He does however give an estimate of the risk in the differently coloured Swiss hazard zones and his numbers corroborate our findings to a degree.

This report is a thorough revision of an earlier report (Jónasson and Arnalds 1997) and our work on avalanche transfer methods has been described in (Sigurðsson et al. 1998). Several other reports have been written during the course of the method development, but these are all in Icelandic and we do not include them in our reference list. We wish to thank our primary collaborators, Gunnar G. Tómasson, Kristín Friðgeirsdóttir, Harpa Grímsdóttir and Tómas Jóhannesson.

In Chapter 2 we discuss risk and its measurement, address the question of what level of risk should be deemed acceptable, and mention the connection between risk and avalanche return period. In Chapter 3 the idea of transferring avalanches between paths is developed. In Chapter 4 we define runout indices and describe how their distribution may be calculated. From this distribution the distribution of runout distances is readily obtained. Chapter 4 also discusses the need to correct the calculated runout index distribution by estimating the proportion of avalanches recorded at each runout index and a rudimentary approach to estimating this proportion is described. In Chapter 5 we discuss survival probability, and estimation of local frequency in Chapter 6. Finally, in Chapter 7, the threads are tied together and formulae for calculating avalanche risk are presented. Chapter 7 also discusses some of our experimentation with the methodology, including examples of its use in two Icelandic towns.

2 RISK

Sometimes the word *risk* is used to mean hazard that has been measured or quantified and we shall use it in this sense here. We shall in this chapter discuss risk and explain why we base our hazard zoning method on estimating the probability of being killed in an avalanche. We also discuss how high an avalanche risk should be tolerated.

2.1 Measures of risk

Before embarking on the measurement of risk one must agree upon a unit to use. There are several possible definitions of this unit. One might measure the return period of avalanches, the expected value of property lost in avalanches (economic risk), the expected number of people killed in the area in a given time period, and finally one can measure individual risk as the annual probability of being killed in an avalanche if one lives or works in a building under a hazardous hillside. The last definition is the chosen one, but to make it workable one must first specify the type of building and secondly the proportion of the time spent inside the building. Most of the houses in the avalanche hazard towns in Iceland are fairly weak timber or concrete houses with relatively large windows facing the mountain side. In the work presented here such a house is assumed. As a reference value we then calculate the risk based on the person being present in the building 100% of the time, and refer to this as *calculated risk.* This is the same unit as that chosen in the aeroplane crash risk report (Evans et al. 1997).

2.2 Exposure

The probability of being killed is found by multiplying the calculated risk with an estimate of the *exposure*, that is, the probability that the person is at home or at work when the avalanche strikes. The exposure depends on the age of the person and the type of the building. For living houses it might be as high as 75% for children but lower for adults. For work places it is lower than for houses, maybe about 30%, and it will be lower still in summer cottages (often less than 5%). This difference is the main reason for not including the exposure in the calculated risk.

2.3 Acceptable risk

Associated with risk measurement is the concept of acceptable risk. Having estimated the risk at each point in a given area the risk value considered acceptable will define the limits of the hazard zones. A common method of determining the acceptable risk level due to a particular hazard is to compare it with other risks. Following the 1995 accidents the acceptable level of avalanche risk has been much discussed in Iceland and regulations for the assessment of avalanche hazard and utilisation of risk areas have been under construction. This work is now in the final stages and the proposed regulations state that for living houses the calculated risk level $0.3 \cdot 10^{-4}$ is acceptable, for work places $1 \cdot 10^{-4}$ and for summer cottages $5 \cdot 10^{-4}$. For Icelandic children aged 1–15 years the yearly death rate from all causes is approximately $2 \cdot 10^{-4}$, about half of this is due to accidents and the other half due to illness. About 40% of the fatal accidents are traffic accidents. Assuming a 75% exposure the avalanche hazard on the acceptable risk line will add $0.225 \cdot 10^{-4}$ or 11% to the death rate of children. In areas carrying this risk the expected number of children killed in avalanches will be about half of the expected number of traffic victims. This comparison assumes that children are as likely as adults to be killed by avalanches, which has been the case in Icelandic avalanche accidents. The acceptable risk for work places has been justified by a similar comparison. It is higher than for homes both because the exposure at work places is lower than at homes and because the adult

death rate is higher than for children. We summarise these numbers along with a few added details in Table 1.

Type of building	Acceptable risk	Deciding age group	Annual death rate	Exposure	Increase in death rate due to avalanche hazard		Assumption behind death rate increase
					Absolute	Relative	
Living house	$0.3 \cdot 10^{-4}$	1-15 yrs	$2 \cdot 10^{-4}$	75%	$0.22 \cdot 10^{-4}$	11%	The school is safe
Work place	$1 \cdot 10^{-4}$	15-30 yrs	$7 \cdot 10^{-4}$	30%	$0.48 \cdot 10^{-4}$	7%	The home is on a $0.3 \cdot 10^{-4}$ line and 60% of the time is spent there
Summer cottage	$5 \cdot 10^{-4}$	1-15 yrs	$2 \cdot 10^{-4}$	5%	$0.25 \cdot 10^{-4}$	12%	The home and the school are safe

Table 1.   De*tails of acceptable risk.*

2.4 Return period as a measure of risk

In Norway regulations state that new houses shall not be built where avalanches fall more frequently than once every 1000 years (Lied 1993). In Switzerland the limit of the hazard zone is set at the tip of a 300 year avalanche (Salm et al. 1990), but the Swiss return periods are not entirely comparable to the Norwegian ones. Firstly, the avalanche may pass the house without hitting it and secondly the runout distance of the 300 year avalanche is in practice calculated from an estimated 300 year maximum of 3 day snow fall in the starting zones and this extreme snow fall does not necessarily produce an avalanche each time. In fact there are some grounds to believe that the actual limits of the hazard zones both in Norway and in Switzerland correspond to a return period somewhat higher than 1000 years (meaning that a house on the limits will be hit by an avalanche more seldom than once every 1000 years).

The relation between avalanche frequency and risk depends on several things. The two most important factors are probably hill height (and thus size and speed of a big and rare avalanche from the hill) and frequency of avalanche release. To name a few other determinants, path confinement, aspect of the hillside and slope of the starting zone might also affect this relation.

For a very low hill most avalanches are not very deadly. One can easily envisage a house under a low hill which is hit or touched by a small avalanche every 500 years, but the risk of being killed in avalanches hitting the house is so low that the house is actually on the acceptable ($0.3 \cdot 10^{-4}$) risk line. Under high hills we would expect the risk on the 500 year line to be much higher.

We shall see in Section 7.5 that the $0.3 \cdot 10^{-4}$ risk line as given by the method described in this report corresponds on average to about the 5000 year line. For the currently used runout index distribution this varies greatly depending on the frequency of avalanches and can for high hillsides range from 3000 years where avalanches are more frequent to 7000 years or more for hillsides where avalanches seldom fall. This variability indicates that return periods are not a good unit for measuring risk, and this assertion is reinforced by the fact that using return periods makes comparison with other hazards difficult.

3   TRANSFERRING AVALANCHES BETWEEN PATHS

One of the major tasks in hazard zoning is estimating the possible runout distances of avalanches that come very seldom indeed as the numbers of the previous section indicate. Avalanche records in most of the housing areas under consideration in Iceland only go back about 100 years and therefore it is impossible to base the frequency estimation of long avalanches that come every several thousand years on local history alone. By combining the avalanche

history of many paths one may however imagine that one path has been observed for a long time rather than many paths for a short time. To make this possible one must be able to tell how far an avalanche that has fallen in a given path would reach in another path. In other words one needs a method that enables the transfer of avalanches between paths.

This concept is developed in Sigurðsson et al. (1998). In particular, the Norwegian alpha-beta model, as well as the runout ratio method of McClung referred to in the introduction may be considered as examples of *topographical* transfer methods. Jóhannesson (1998b) has developed an alpha-beta model for Icelandic avalanches and fitted runout ratios to a Gumbel distribution using the longest avalanches in each path. As also mentioned in the introduction Keylock (1996) has constructed a similar runout ratio fit for Icelandic avalanches, where he takes into account all known avalanches in each path, rather than just the longest one. An alpha-beta model for Austrian avalanches is discussed by Lied et al. (1995).

By contrast we have developed so-called transfer methods based on *physical* models. One of the advantages of using a physical model to transfer avalanches is that it enables direct estimation of the speed profile of an avalanche, i.e. its speed at each point along its path, which in turn is needed for the calculation of risk. Some authors (e.g. McClung 1990) have argued that due to the sensitivity of runout distances calculated by physical models to changes in the parameters one should first use topographical methods to estimate runout distances and then use physical models for speed estimates. By using physical models to transfer runout distances from a large data set and then treating the transferred values statistically, this sensitivity is however less of an issue.

3.1 The avalanche data set

We have worked with a data set of 196 avalanches recorded in Iceland. The data were compiled by Kristín Friðgeirsdóttir at the University of Iceland in 1995–1996. The avalanches fell from 81 different paths in about 50 different hillsides, and 34 of the avalanches fell into the sea. The oldest ones fell just over 100 years ago. Some of the paths have a shorter observation history and it cannot be far off to guess that the average observation period is about 80 years. The data set contains 23 pieces of data about each avalanche, for instance path name, date, stopping position and width. The path profile is also recorded. The data set is based on avalanche maps and lists obtained from the Icelandic Meteorological Office, covering 8 Icelandic towns and villages. All avalanches shown on these maps were included in the data set. The maps cover the period until 1989, though a few later avalanches were also included.

3.2 Avalanche transfer by the PCM model

Our physical transfer methods have so far been based on the simple PCM model for avalanche flow, with two free parameters, the Coulomb resistance parameter μ, and the mass-to-drag parameter M/D (see Perla et al. 1980). It should be noted, however, that we separate the curvature term, κ, from the M/D term in the PCM model, i.e. the differential equation of the model is

$$\frac{1}{2}\frac{d}{ds}(u^2) = g(\sin\theta - \mu\cos\theta) - (\mu\kappa + \frac{1}{M/D})u^2$$

where u denotes the speed of the avalanche, s the distance along the path, θ its slope and g the gravitational acceleration. The equation is solved numerically from its integral representation. The θ-value at distance s is taken to be the mean slope between distances $s - L/2$ and $s + L/2$

for a specified reference length L. The radius of curvature, $1/\kappa$, is the radius of the circle tangent to the lines between distances $s - L/2$ and s on one hand and s and $s + L/2$ on the others, at their midpoints. The calculation starts at distance $L/2$ from the estimated avalanche breakline, and the end of the avalanche is taken to be at distance $L/2$ beyond the calculated stopping point. For the present study we have taken L to be 75 m in all cases.

The determination of the input parameters, μ and M/D, is difficult because an infinite number of pairs can explain a given avalanche runout in a given path. Increased friction can be compensated by increased mass-to-drag (decreased drag). The curves in Figure 1 represent different pairs of coefficients that can explain a few avalanches in the Icelandic data set. Such a curve is called an *isorunline* for the corresponding avalanche.

In the case of an avalanche falling into the sea, the isorunline corresponds to the seashore, and any parameter pair between the isorunline and the M/D-axis may explain the avalanche.

The complication of several different parameter pairs explaining a given avalanche can be overcome by selecting a line of likely parameter pairs through the parameter space. This line is called the *parameter axis*. The intersection of the parameter axis and the isorunline of an avalanche gives the parameter pair used to explain the avalanche. Figure 2 shows the parameter axis that we have used and the isorunlines for all 196 avalanches in the data set. If the runout distances of two avalanches in different paths can be explained by the same parameter pair (i.e. if the corresponding isorunlines intersect the parameter axis in the same point) then the two runout distances are considered to be equivalent, and one can be transferred to the other. By a classification scheme introduced in Sigurðsson et al. (1998) we refer to this transfer method as a PCM-1 method. Using a parameter axis in this way means that a single parameter pair corresponds to each runout distance and through the PCM model a unique speed profile is obtained for an avalanche stopping there.
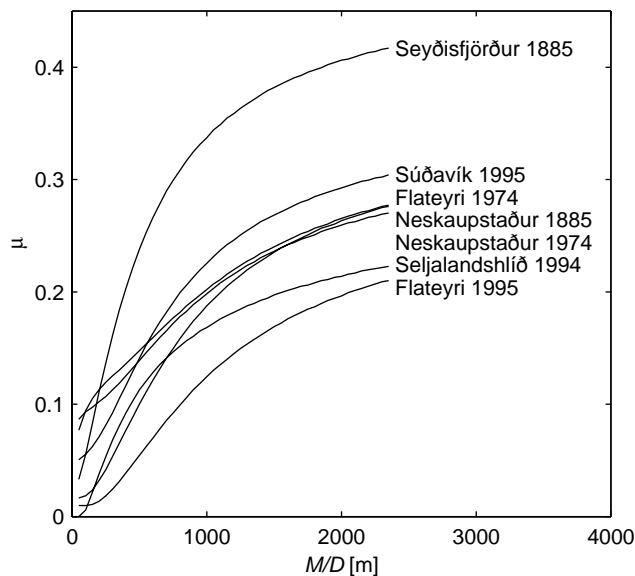

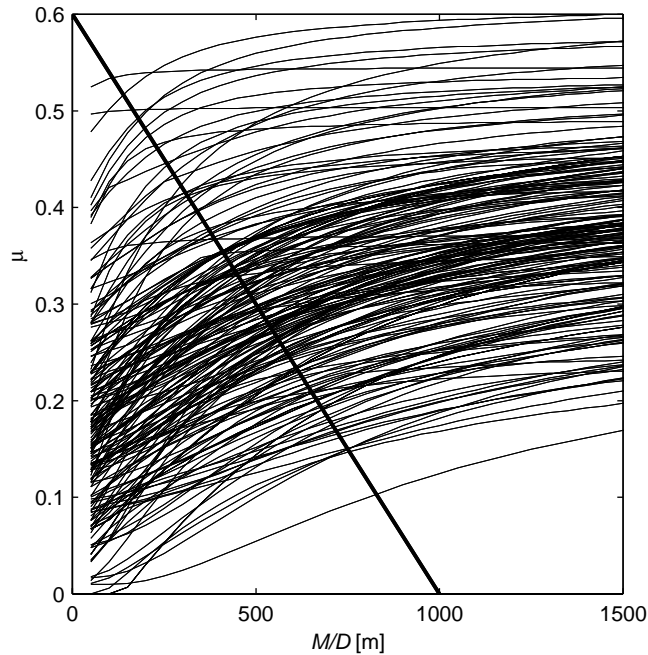Figure 1. *Isorunlines for a few well known Icelandic avalanches.*

Figure 2. *Isorunlines for 196 Icelandic avalanches and the parameter axis.*

Another way of justifying the use of a parameter axis is as follows: Assume that the parameters μ and *M/D* follow a joint probability distribution that is independent of the avalanche path, and that when an avalanche falls, its properties are determined by selecting parameter values at random from this distribution. The probability that an avalanche travels further than a given runout distance, its *runout probability*, will be given by the fraction of the probability mass of the distribution that is between the corresponding isorunline and the *M/D*-axis. Two avalanches will be equally likely if their runout probabilities are the same. The most likely parameter pair explaining an avalanche will then be the maximum point of the joint density function on the isorunline of the avalanche. We could select a parameter axis that approximates the locations of these maximum points for all avalanches in a collection. Because the isorunlines are approximately parallel this choice of parameter axis will ensure that two avalanches with equal runout probabilities will be approximately equivalent, in the sense that the points of intersection between their isorunlines and the parameter axis will lie close to one another.

It is possible to use runout probability to define the equivalence of avalanches and base the transfer method on that. In Sigurðsson et al. (1998) we refer to such an approach as a PCM-3 transfer method. The parameters of an appropriate bivariate parameter distribution can be estimated from the isorunlines using maximum likelihood criteria. Furthermore one can take into account in a consistent manner the case where additional measurements of an avalanche restrict the choice of parameters that can explain its runout distance. We have tried this idea out on the questionable assumption that the underlying distribution is bivariate normal, using data on avalanche depth in the starting zone to fix the parameter pair for a few avalanches on the equally questionable assumption that the *M/D*-parameter is proportional to that depth. However, it turns out to be crucial for the stability of the maximum likelihood estimation method to have some such fixed pairs. Thus this approach has yet to lead to reliable estimates of the parameter distribution. Another possibility of fixing the parameters would be to make use of direct or indirect speed measurements of an avalanche, since different parameter pairs on the same isorunline correspond to different speed profiles. But even if more reliable esti-

mates could be obtained it seems doubtful that the extra computational effort in the PCM-3 transfer method would be justified in terms of increased accuracy. Better parameter estimates would, however, be valuable for identifying an appropriate parameter axis in the PCM-1 method, as discussed below.

3.3 Choice of parameter axis

In the absence of a reliable parameter distribution estimate, we may turn to the literature to see what parameter values have been used elsewhere in avalanche simulations with the PCM model. These simulations usually deal with the longest recorded (or longest "likely") runout distance in a path. Perla et al. (1980), introducing the PCM model, used data from Canada and USA and suggested that μ should be in the range 0.1 to 0.5 and M/D in the range 100 to 10000 m. More recently McClung (1990), taking a somewhat different view of the physical assumptions behind the model, suggests that the μ-values may exceed 0.5 and that typical M/D-values are in the upper part of the bracket. Workers at NGI deduce from simulations of avalanches in Norway and Austria that typical μ-values are in the interval [0.15, 0.35] and that for avalanches in Norway one should set $M/D = 0.5 \cdot H$ and for those in Austria $M/D = 0.8 \cdot H$, where H denotes the height of the path, typically in the range from 600 to 1200 m (Lied et al. 1995). Finally, in the analogous VSG-model used in Switzerland the value of μ ranges from 0.155 for large dry avalanches to 0.30 for wet ones, and while the model is not based on a fixed M/D-parameter the corresponding values are typically in the range from 200 to 600 m (Salm et al. 1990).
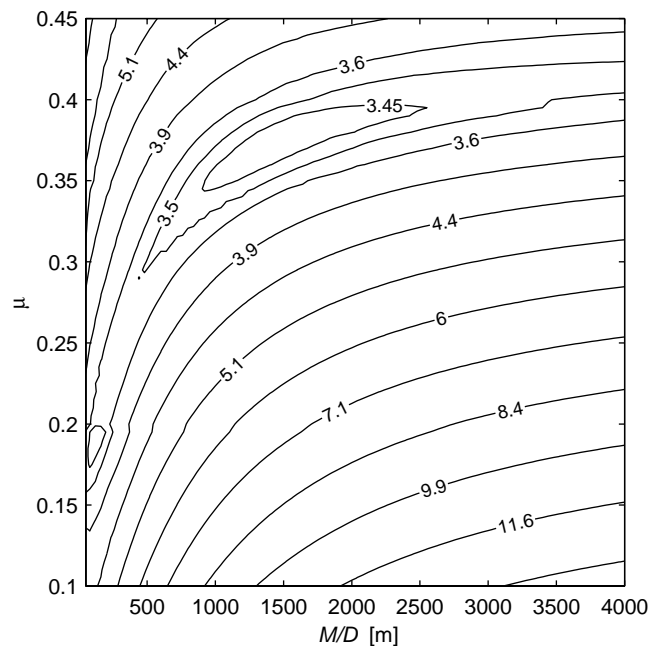
Figure 3. *Root mean square deviation between PCM-predicted α-value and recorded α-value.*

For the Icelandic data set and for different (M/D, μ)-parameter values, we have calculated the mean square deviation between the actual α-angle of a runout distance and the α-angle calculated with the PCM model ($\alpha = \arctan(H/x)$ where H denotes the height of the avalanche and x its horizontal runout distance). Avalanches falling into the sea have been "spread over the sea" in a manner consistent with the assumption that these deviations are normally distrib-

uted. As an example of such spreading, see Jóhannesson (1998b). The results are shown in Figure 3 where the contour lines are marked with the square-root of the corresponding mean square deviation (in degrees). The minimum occurs at approximately $(M/D, \mu)$ = (1500 m, 0.375). These values are somewhat high compared with those quoted from the literature, but it should also be noted from the figure that the mean square deviation will not increase significantly if the parameters values are decreased to e.g. (500 m, 0.30). Furthermore the sensitivity of changes in α-values to changes in the parameter values differs between slopes, and ideally this should be taken into account by introducing suitable weights for the deviations (with less weight on the slopes where the sensitivity is large). An advantage of the maximum likelihood estimation referred to in the previous section is that it implicitly takes care of this.

Guided by all these considerations the parameter axis has been chosen to go through $(M/D, \mu)$ = (500 m, 30) with the equation

(1)
$$\mu = 0.6 - 0.0006 \; M/D.$$

On this axis the avalanches in our data set range between $(M/D, \mu)$ = (109 m, 0.534) and (828 m, 0.103). Some typical values of $(M/D, \mu)$ on the axis are presented in Table 2.

M/D	100	150	200	250	300	350	400	450	500	550	600	650	700	750	800	850
μ	0.54	0.51	0.48	0.45	0.42	0.39	0.36	0.33	0.30	0.27	0.24	0.21	0.18	0.15	0.12	0.09

Table 2. *Pairs of (M/D, μ) on the parameter axis.*

For comparison two other parameter axes were tried, one of them going through the minimum point referred to above, and the effect on hazard estimates was calculated. This comparison is detailed in Section 7.4.

For simplicity's sake we have chosen to use a straight line for the parameter axis. A disadvantage of using a straight parameter axis is that extremely long or short avalanches cannot be explained, because their isorunlines will not intersect the axis. A better choice may be a hyperbola-like line that would asymptotically approach the μ-axis for small M/D and the M/D-axis for small μ. Note however that all 196 avalanches in the collection can be explained by the chosen straight parameter axis.

It should further be noted that in the absence of the curvature term and the drag term in the PCM model, the ratio between the calculated height of the avalanche, H, and the calculated horizontal runout distance, x, will simply be μ. The implication is that if the parameter axis is chosen far to the right (corresponding to large M/D) the length of an avalanche will simply be characterised by its α-angle.

4   RUNOUT INDICES

4.1 The standard path

To accomplish a descriptive uniform runout distance scale a *standard path* that is representative for the Icelandic (and to some extent Norwegian) avalanche paths has been defined. An avalanche can be transferred to the standard path, and the (horizontal) runout distance there measured in hectometres defines the runout index of the avalanche. The standard path is shown in Figure 4. It is parabola shaped, 700 m high and reaches level ground 1600 m from the starting point. The equation for it is

$$y = \begin{cases} \dfrac{700}{1600^2}(x-1600)^2 & \text{if } 0 \le x \le 1600 \\ 0 & \text{if } x > 1600 \cdot \end{cases}$$

To calculate the runout index of an avalanche, find the (M/D, μ) pair on the parameter axis that makes the PCM simulated avalanche stop in the correct place. A simulated avalanche with this parameter pair is then initiated at the top of the standard path, and its stopping position gives the runout index. Table 3 contains a list of the 10 avalanches in the data set with the highest runout indices.
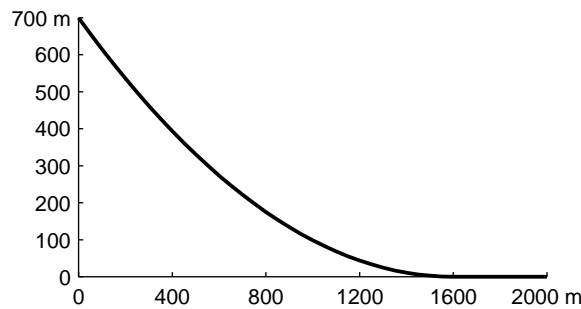

Figure 4. *The standard path.*

Town	Path	Year	Runout index
Flateyri	Skollahvilft	1995	18.8
Ísafjörður	Seljalandsdalur, old ski hut	1994	17.0
Flateyri	Skollahvilft	1953	16.9
Flateyri	Innra-Bæjargil	1974	16.9
Neskaupstaður	Brynjólfsbotnagjá	1936	16.9
Súðavík	Traðargil	1995	16.6
Neskaupstaður	Gully below Gunnólfsskarð	1990	16.5
Neskaupstaður	Bakkagil	1974	16.4
Súðavík	Traðargil	1994	16.4
Neskaupstaður	Ytri Sultarbotnagjá	1885	*16.3

Table 3. *The ten longest avalanches in the Icelandic data set. The avalanche marked with **
fell into the sea.

4.2 Combined avalanche history

By transferring all the avalanches in the Icelandic data set to a single slope we can imagine that we have a 4000 year observation period there instead of having watched 50 paths for 80 years. Continuing along this track it would be possible to estimate the frequency of avalanches that reach a given runout index by counting the number of avalanches in the data set that have a longer runout after being transferred. For instance, there are 7 avalanches with a runout index of 16.5 or higher giving an average return period of $4000/7 \approx 570$ years.

Such a direct calculation has several flaws. Firstly, the overall frequency of avalanches on different hillsides is different. Even if all of the hills had the same runout index distribution and all avalanches with runout index above 16.5 have been recorded, the above calculation will

only be valid on a hill where the frequency of avalanches is equal to the overall average of the 50 hills.

A second flaw is that not all avalanches on the slopes in the data set during the last 80 years have been recorded, and the recording of avalanches is not uniform. A long avalanche is more likely to have been recorded than a short one. This is the problem of the *missing avalanches*, dealt with in Sections 4.3 and 4.4.

Third, some of the avalanches have gone into the sea. For these avalanches, all we know is that their runout index has exceeded the runout index at the foreshore. This problem is technical and not very difficult. It has been solved by "spreading the avalanches over the sea" in a consistent manner.

Fourth and finally, the runout index distribution need not be the same in all the hillsides. Even if the overall frequency in a path is high, it does not necessarily follow that the frequency of long avalanches is also high. For some avalanche paths a long runout might be impossible. In our present approach this problem has simply been ignored and a global runout index distribution has been assumed, one that we apply to every high hillside in Iceland. The data available are not extensive enough to classify the hillsides and estimate separate distributions for the different classes.

4.3 Distribution of runout indices

Using a statistical procedure known as *kernel estimation* (e.g. Silverman 1986), the combined history of avalanches after transfer to the standard path can be used to estimate a probability distribution of runout indices. Figure 5 shows the estimated density function with a histogram of the runout indices superimposed. Kernel estimation can be thought of as a smooth histogram of the data. The degree of smoothness depends on the width of the basis kernel function and after some experimentation a Gaussian basis function with standard deviation of 0.75 runout indices was selected. The reason the density function lies above the histogram near the right end is that in the histogram sea avalanches are recorded as stopping at the coastline, whereas in the density function they have been "spread over the sea" in a manner consistent with the derived distribution. Because of incomplete recordings of shorter avalanches the real distribution of runout indices is quite different from the one shown in Figure 5. To emphasise this we refer to the density function shown in Figure 5 as the *data density* and the corresponding distribution as the *data distribution*. We denote the data density function by $f_D(r)$.

In order to obtain the density function of the real distribution of runout indices, first note that we shall only be interested in the shape of this function for *r* above some suitable *base index* R_0. Thus we only need to estimate the probability of an avalanche with index *r* being recorded when $r \geq R_0$, and we refer to this probability as the *recording proportion* at *r*. We further distinguish between the global recording proportion, which applies to the whole data set and is denoted by $p(r)$, and the local recording proportion in a particular path, denoted by $q(r)$. The local recording proportion comes into play in Chapter 6, when estimating avalanche frequency. The real distribution of runout indices of avalanches reaching index R_0 is given by

$$(2) \qquad f(r) = \frac{1}{\int_{R_0}^{\infty} f_D(t)/p(t)\,dt}\, f_D(r)/p(r).$$
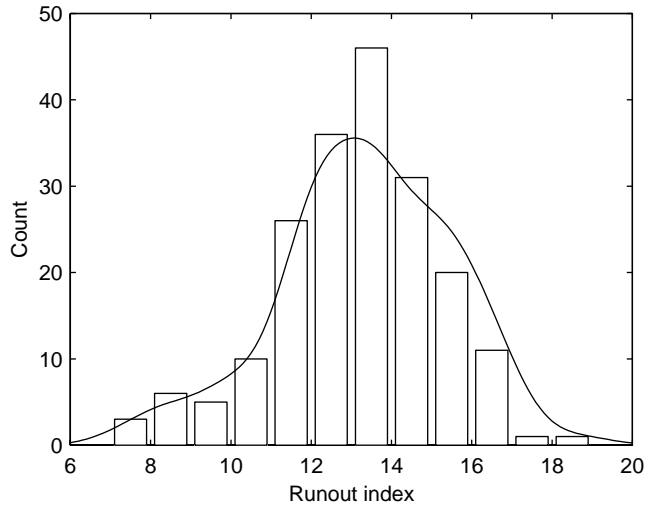
Figure 5. *Runout indices of 196 Icelandic avalanches together with kernel estimated data density function.*

The function f does of course depend on R_0. The *exceedance probability* that an avalanche exceeding R_0 will also exceed $r \geq R_0$ is given by

$$(3) \qquad\qquad E(r) = \int_r^\infty f(t)\,dt$$

where again the dependence on R_0 is tacit. While the appropriate value for R_0 may vary, it is convenient for the presentation to fix a particular value, and we have chosen to set $R_0 = 13$. Note that this means that $E(13) = 1$.

We believe that the most reliable approach to obtaining the recording proportion in the main hazard areas in Iceland is to use records of when houses were built. Physical evidence of avalanches like broken trees is scant in Iceland, and until recently historical records of avalanches have generally been restricted to those causing death or significant damage. We believe, however, that the records for the last century are relatively complete for avalanches with a runout index above 16.
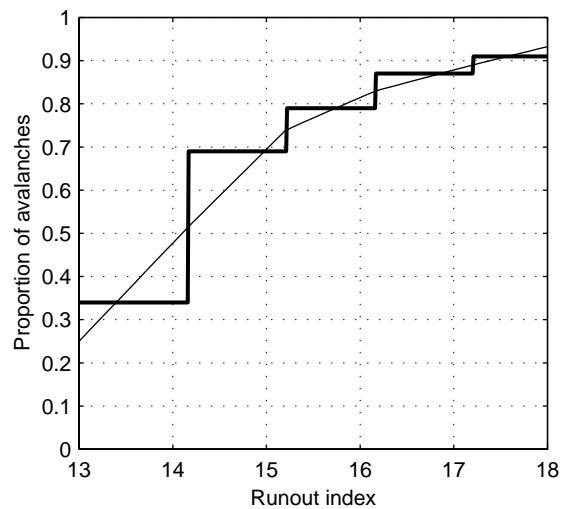

Figure 6. *Estimated proportion of recorded avalanches in Neskaupstaður, based on age of houses. The narrow line is simply a smoothing of the staircase graph.*

18

We illustrate our approach by considering the town Neskaupstaður where such housing data have already been prepared (Grímsdóttir 1998). There are 7 main avalanche paths with 20 recorded avalanches of runout index 13 or higher in the last century. Taking the age of individual houses under each gully into account we have estimated the local recording proportion $q(r)$ and the result is shown in Figure 6. To indicate how this was done, assume that a century ago two houses were under a gully at runout index 16 and that these were the only houses under the gully until 1950. Then a dense row of houses was built at runout index 14. The likelihood of avalanches beyond 16 having been recorded in the first 50 years is thus high, 80% say (the avalanche may have bypassed the houses without causing damage), but low if they are shorter, 20% say for avalanches with indices 15–16 and 0% for even shorter ones. In the second 50 years, when recordings were more systematic and not as restricted to avalanches causing damage, we may assume that all avalanches beyond 14 have been recorded, and 80% of those with indices 13–14. Assuming a uniform frequency of avalanches with time, the overall estimate for the 100 year period would be that beyond 16, the recording proportion is 90%, and between 15 and 16, it is 60%. From 14 to 15 it is 50%, and 40% between 13 and 14. We shall not go into further details of how the estimate is obtained.

When similar housing data have been compiled for all the other main potential hazard areas we shall be able to estimate $p(r)$ by averaging locally estimated recording proportions weighted with the number of recorded avalanches in each path. In the meantime we may resort to a more rudimentary approach that we describe in the next section.

4.4 Rudimentary estimate of global recording proportion function

We have used data on avalanches in Flateyri and Neskaupstaður, which both have relatively many recorded avalanches, to estimate the recording proportion function p. For Flateyri we can utilise the work of Jóhannesson (1998a) where he estimates the distribution of runout distances for all avalanches from the Skollahvilft avalanche path, the location of the catastrophic 1995 avalanche. For Neskaupstaður, on the other hand, we use the estimate of the local recording proportion, $q(r)$, discussed at the end of the previous section, together with the distribution of recorded avalanches, to obtain a distribution of runout indices for all avalanches. Having obtained these two separate estimates of the density function for all avalanches, $f(r)$, we proceed to assess $p(r)$ using (2).

In Flateyri 14 avalanches with a runout index greater than 14.5 are recorded from the Skollahvilft path. For this path, the avalanche records are believed to be fairly accurate for runout indices greater than 14.5 and some information about the frequency of avalanches in the runout index interval 13–14.5 is also available. Jóhannesson fits a Gumbel distribution to the longest yearly runout distance and obtains the distribution function

$$(4) \qquad D(x) = e^{-e^{-(x-a)/b}}$$

where x is horizontal runout distance, $a = 1354$ and $b = 97$. For our purpose we need to measure the runout distance using runout indices. Using the data in Table 4 and linear regression in the interval [14,20] we have changed the distribution (4) to depend on runout index and obtained the distribution function

$$(5) \qquad D_{\text{Flat}} = e^{-e^{-(r-a)/b}}$$

now with a = 13.3 and b = 0.925. The corresponding density function is

$$f_{\text{Flat}}(r) = D_{\text{Flat}}(r)\, e^{-(r-a)/b}/b$$

and this is shown with a dashed line marked 'Flateyri' in Figure 9. Incidentally, (5) also gives us a frequency estimate for Skollahvilft avalanches reaching $r = 13$, namely $F_{13} = 1 - D_{\text{Flat}}(13)$ = 0.754 avalanches per year.

Runout index	13.0	13.5	14.0	14.5	15.0	15.5	16.0	16.5	17.0	17.5	18.0	18.5	19.0	19.5	20.0
Runout distance	1309	1374	1425	1471	1537	1591	1638	1686	1737	1790	1842	1896	1950	2004	2059

Table 4.   *Runout index vs. runout distance in Skollahvilft, Flateyri.*

For 7 main gullies in Neskaupstaður, as said in the previous section, we have data on 20 avalanches with $r \geq 13$. Table 9 in Section 6.2 lists these avalanches. We use kernel estimation to obtain the data density of the runout index of these avalanches in the same way as in Section 4.3 and the result is shown in Figure 7. As in Section 4.3 we have taken into account in an appropriate way the fact that three avalanches went into the sea.
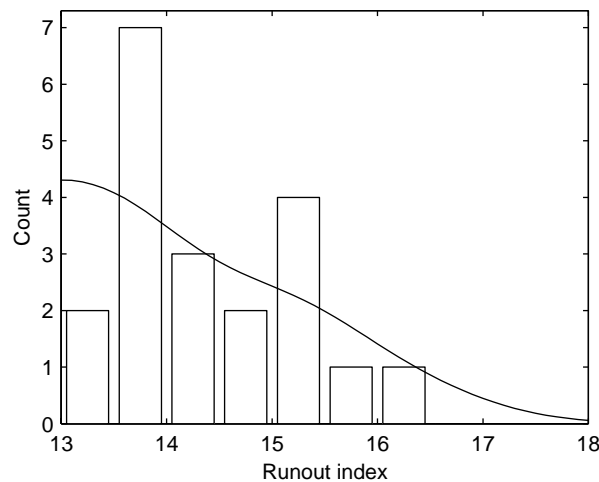

Figure 7. *Distribution of runout indices of 20 avalanches from 7 gullies in Neskaupstaður together with kernel estimated density function.*

If we divide this density function by the smooth curve of Figure 6 and normalise, we obtain the estimate $f_{\text{Nesk}}(r)$ of the density of all avalanches shown with a dash-dotted line labelled 'Neskaupstaður' in Figure 9.

By (2) the recording proportion, $p(r)$, is equal to $f_D(r)/(Kf(r))$ where K is a constant. We find that for $f(r) = (f_{\text{Flat}}(r) + f_{\text{Nesk}}(r))/2$ the function $1/p(r)$ is well described by a shifted normal density function of the form $1 + a\phi((r - \mu)/\sigma)$, where ϕ is the standard normal density. Note that it is natural to select a function that tends to 1 as r goes to infinity. We have determined a, μ and σ by restricting the fit to the runout index interval [13,18] and this gave $a = 95.5$, $\mu = 10.6$, $\sigma = 2.34$ and $K = 4.98$ (note that K is not really a free parameter because given values of a, μ and σ we may use (2) to determine K). Figure 8 and Figure 9 show the resulting fit.
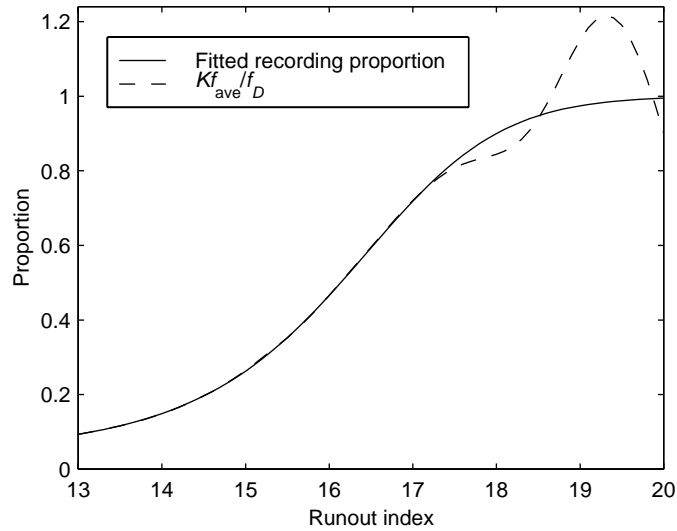
Figure 8. *Recording proportion estimated from Flateyri and Neskaupstaður data together with a smooth fit.*
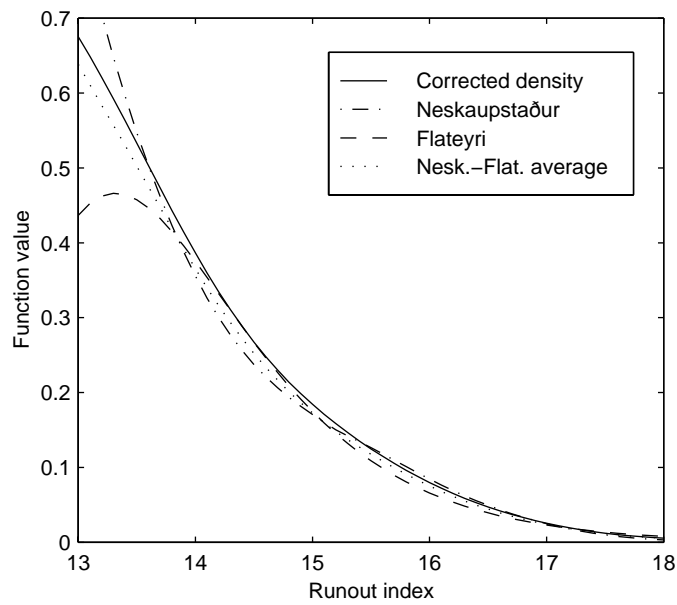

Figure 9. *Runout index density functions for Flateyri, Neskaupstaður, average of these and corrected density found by smoothing the Neskaupstaður-Flateyri recording proportion.*

Table 5 lists the exceedance probabilities (3) for a few selected runout indices, together with corresponding exceedance probabilities for the data density function f_D.

Runout index, r	Exceedance probability Data distribution	Exceedance probability Corrected distribution
13	100.00%	100.00%
14	69.35%	46.76%
15	43.07%	19.41%
16	21.33%	6.69%
17	7.40%	1.78%
18	2.09%	0.44%
19	0.62%	0.13%
20	0.10%	0.02%

Table 5. *Runout index exceedance probability. Conditional probability that an avalanche reaches runout index r given that it reaches r = 13. The second column applies to recorded avalanches and the third column to all avalanches.*

Keylock (1996) estimates the exceedance probability of Icelandic avalanches as a function of runout ratio. A rough way of relating runout ratios and runout indices is to use the position of the β-point of the standard path, i.e. the point where the slope is 10°, which is at 1278 m horizontal distance from the start. This gives

$$(6) \qquad \text{runout ratio} \approx \frac{\text{runout index}}{12.78} - 1.$$

In Figure 10 we reproduce the graph of Figure 2.12 of Keylock and superimpose our corrected exceedance probability, calculated with (6) and multiplied so that the percentages agree for $r = 13$. As an example of what can be read from this figure, our estimate of the proportion of $r > 13$ avalanches that reach $r = 18$ is about ¼ that of Keylock (at $r = 18$ our line is about 0.6 grid-line interval below Keylock's line and $1/10^{0.6} \approx 1/3.98 \approx$ ¼).
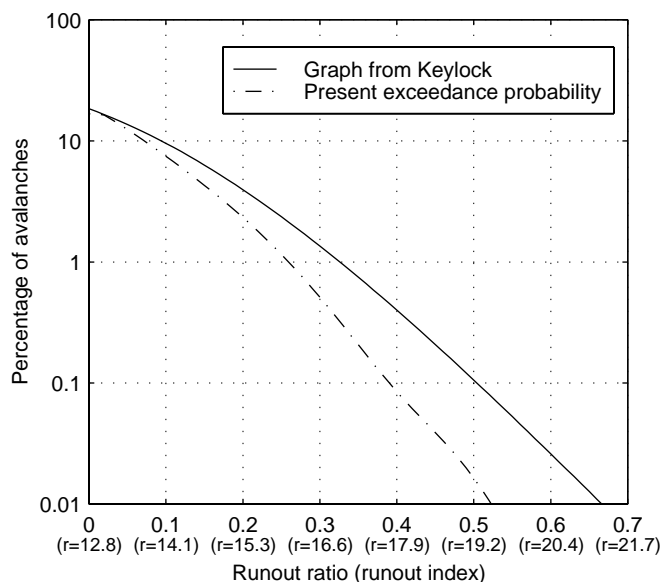

Figure 10. *Comparison of present estimate of exceedance probability as a function of runout ratio with the estimate of Keylock (1996).*

5 SURVIVAL PROBABILITY

In this section we consider the probability of surviving an avalanche striking a house. In fatal avalanche accidents in Iceland the overall survival rate has been about two thirds. The probability of surviving is obviously not constant, it depends on the speed of the avalanche, and probably other factors such as its wetness and size. Until now we have concentrated on the dependence on speed, and ignored other factors. This does not mean that we believe their effect to be negligible, in fact some dependence of survival on avalanche size is high on our list of possible improvements to the method.

5.1 The avalanches of Súðavík and Flateyri

The probability of a person surviving inside a house when an avalanche strikes at a given speed has been estimated using data from the avalanches of Súðavík and Flateyri. These avalanches damaged a total of 32 houses where 93 people were staying. Figure 11 and Figure 12 show the deposit outlines of both avalanches, the centre line of the avalanche path, and the direction of the avalanche flow (dashed lines with arrows). House numbers are shown for each house where people were staying at the time of the accident. The unnumbered houses inside the avalanche deposit were empty, and thus do not contribute to our estimate of the survival probability.
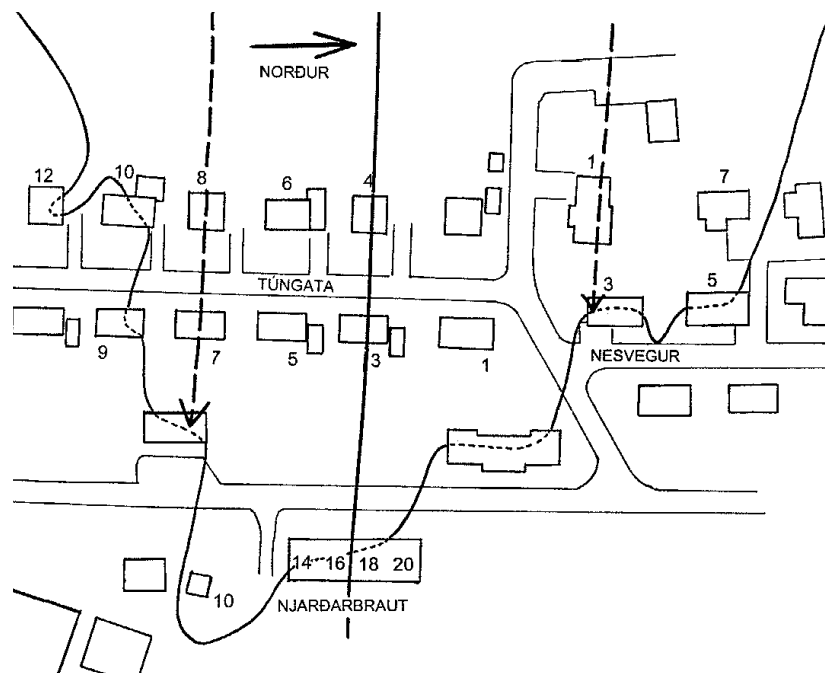

Figure 11. *The outline of the 1995 avalanche on Súðavík and the centre line of the avalanche profile. See Table 7 and main text for details. The drawing scale is 1:2500.*

Flateyri	x [m]	0	75	175	250	350	425	500	575	675	750	800	875	975	1050	1200	1300	1425	1525	1600	1800
	y [m]	638	578	508	455	395	361	326	287	240	221	198	166	132	106	64	41	22	10	6	3
Súðavík	x [m]	0	25	125	175	225	275	350	400	450	500	550	625	700	750	800	925	1000	1150	1225	
	y [m]	547	530	445	393	359	328	263	226	192	161	134	98	74	63	51	30	19	9	6	

Table 6. *The profiles of the Flateyri and Súðavík avalanches. The horizontal distance (x) is measured from the avalanche breakline and the vertical distance (y) is height a.s.l. The location of the lowermost parts of the profiles are shown in Figure 11 and Figure 12. In Flateyri (centre of) Unnarstígur 6 is at x = 1791 m and in Súðavík (centre of) Túngata 3 is at x = 1139 m.*

As said previously we estimate the avalanche speed at a house by modelling the avalanches using the PCM model. The profiles of the avalanches are given in Table 6. Ignoring the breaking effect of the house in question and other houses further down, this speed depends on the stopping point of the avalanche directly downstream from the house. To estimate the breaking effect we have assumed that each row of houses that the avalanche passes shortens its runout distance by the same amount. If an avalanche travelling on a flat surface has slowed so much down that the mass-to-drag effect may be neglected, then, according to the PCM model, the remaining distance is proportional to the square of the speed. Because the kinetic energy is also proportional to the square of the speed, our assumption on a fixed shortening of runout distance per row of houses corresponds to assuming that each row of houses reduces the energy of the avalanche by the same amount.

To determine the shortening per house row, we have inspected the detailed shape of the avalanche deposit, paying special attention to places where tongues of the avalanches have travelled between houses, for example between Nesvegur 3 and Nesvegur 5 in Súðavík or between the houses on Ólafstún in Flateyri. Based on this inspection we have decided to use a breaking distance of 20 m per house row (according to the PCM model with parameters on the axis, the avalanche speed 20 m before stopping is about 7.5 m/s). For each house where people were staying we have measured the distance from the centre of the house to the stopping point downstream from the house. We have also counted the rows of houses that the avalanche passes before stopping (including the row of the house in question). Table 7 lists these numbers and also gives an overview of the number of people at home and the number of people killed in the avalanches. The latter numbers were supplied by the local police who also provided the maps showing the avalanche outlines.

The speed shown in Table 7 is our estimate of the speed of the avalanche when it hit the house. It is found by the PCM model using the (μ, M/D) pair on the parameter axis of Section 3.3 that will make the avalanche stop d m downstream from the house, where d is the corrected stopping distance of Table 7.
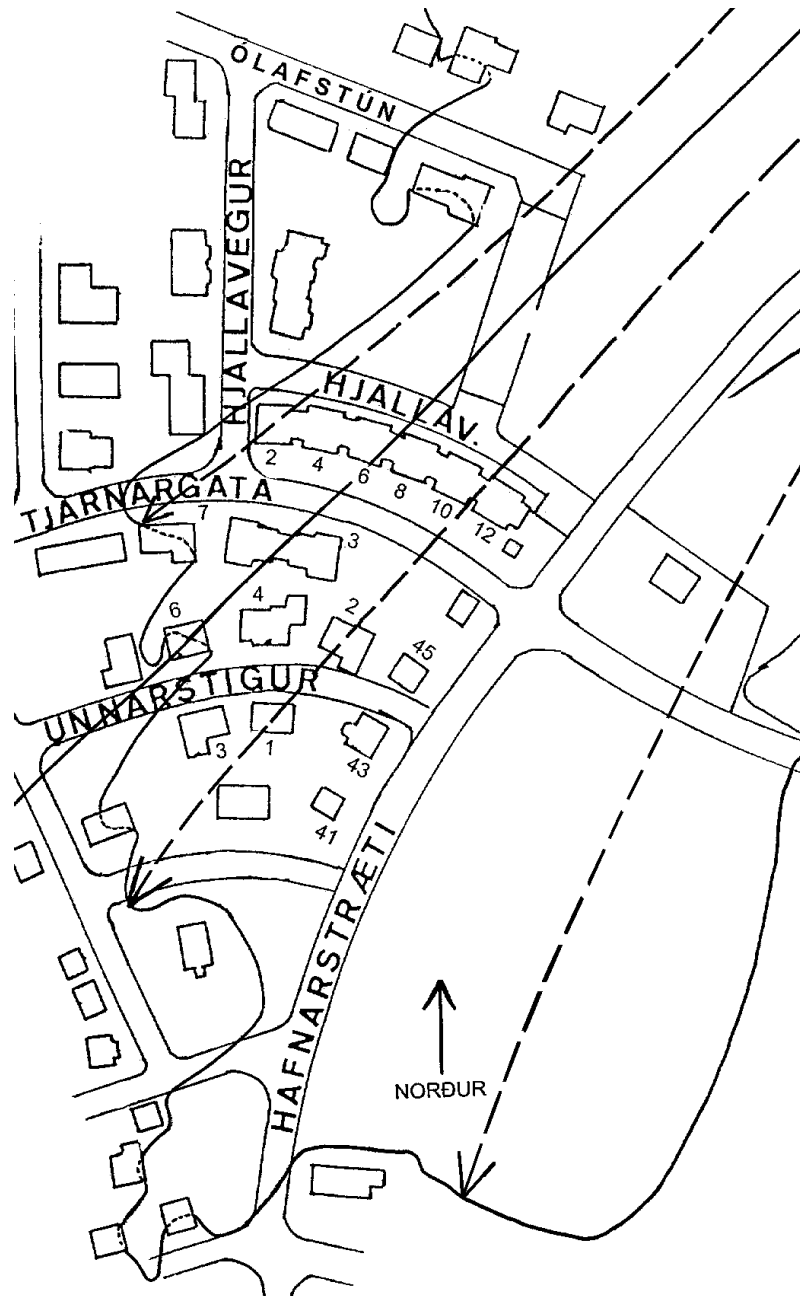
24

Figure 12. *The outline of the 1995 avalanche on Flateyri and the centre line of the avalanche profile. See Table 7 and main text for details. The drawing scale is 1:2500.*

	House	Rest distance [m]	Rows of houses below	Corrected rest distance, d [m]	Avalanche speed [m/s]	People at home	People killed
Flateyri	Hafnarstræti 41	50	1	70	13.5	3	2
	Hafnarstræti 43	75	2	115	17.7	2	0
	Hafnarstræti 45	100	3	160	21.5	3	3
	Hjallavegur 2	60	1	80	15.0	1	0
	Hjallavegur 4	65	2	105	17.3	5	0
	Hjallavegur 6	100	3	160	21.6	1	1
	Hjallavegur 8	150	4	230	26.0	4	3
	Hjallavegur 10	170	3½	240	26.7	5	5
	Hjallavegur 12	170	3½	240	26.7	1	1
	Tjarnargata 3	110	2	150	20.8	2	2
	Tjarnargata 7	0	1	20	7.2	2	0
	Unnarstígur 1	75	1½	105	16.7	5	0
	Unnarstígur 2	115	2½	165	21.7	3	2
	Unnarstígur 3	45	2	85	15.2	4	0
	Unnarstígur 4	90	2	130	19.3	3	1
	Unnarstígur 6	0	1	20	7.1	1	0
Súðavík	Nesvegur 1	35	2	75	15.5	3	0
	Nesvegur 3	0	1	20	7.7	4	0
	Nesvegur 5	0	½	10	6.0	4	0
	Nesvegur 7	30	1½	60	14.4	4	2
	Njarðarbraut 10	20	1	40	10.7	1	1
	Njarðarbraut 18	0	1	20	7.5	1	0
	Túngata 1	35	2	75	15.5	2	0
	Túngata 3	75	2	115	19.2	3	0
	Túngata 4	115	3	175	24.1	4	1
	Túngata 5	100	1	120	18.8	4	3
	Túngata 6	140	2	180	24.1	2	2
	Túngata 7	35	2	75	14.6	4	2
	Túngata 8	75	3	135	20.1	4	3
	Túngata 9	0	½	10	5.2	4	0
	Túngata 10	0	1	20	7.5	1	0
	Túngata 12	0	¼	5	5.2	3	0

Table 7. *Stopping distance, number of breaking house rows, PCM estimated avalanche speed and number of people killed in the avalanches of Flateyri and Súðavík. To correct the stopping distance, 20 m have been added for each house row.*

5.2 Maximum likelihood estimate of the survival rate

Figure 13 shows the fraction of people surviving as a function of speed both by a histogram and by a smooth curve.

The curve is continuously differentiable, and its formula is

(7)
$$s(v) = \begin{cases} 1 - kv^2 & \text{if } v < v_1 \\ c + \dfrac{a}{v-b} & \text{if } v \geq v_1 \end{cases}$$
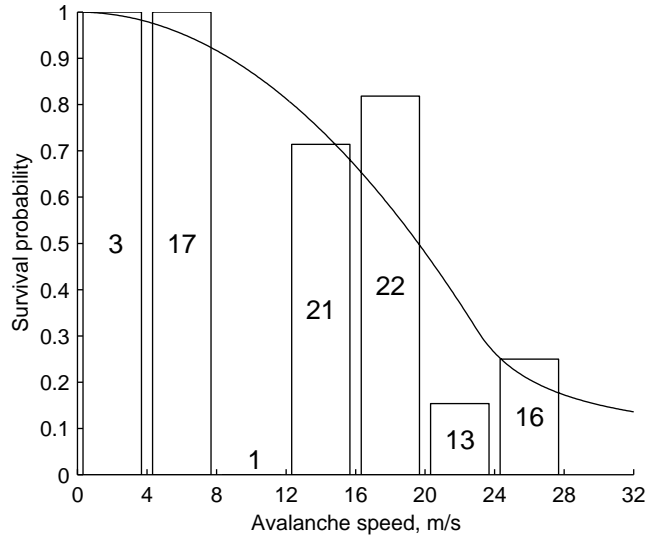
Figure 13. *The dependence of survival rate in Flateyri and Súðavík on the avalanche speed. The numbers in the bars show the total number of people at home for each speed group and the height of the bars gives the proportion surviving. For instance, 25% or 4 people out of 16 survived in the 24–28 m/s speed group.*

where $k = 0.00130$, $c = 0.05$, $a = 1.151$, $b = 18.61$ and $v_1 = 23.0$. The following reasoning has been used for the determination of s. Regarding the form of the formula it is natural to select a decreasing function that asymptotically approaches some constant as $v \rightarrow \infty$. Since the data do not tell us anything about the survival rate for speeds above 27 m/s (the maximum in Table 7) it is necessary to resort to some heuristic estimate for higher speeds. We have assumed that, regardless of how fast an avalanche travels, some proportion of people will always survive. In particular we have in mind people staying in basements at the time of the accident, and also people on upper floors, above the avalanche. This proportion has been taken to be 5%, i.e. $c = 0.05$. The reasons for choosing the survival rate to be of the form $1 - kv^2$ for lower speeds is firstly that the data in Figure 12 indicate such a form, and secondly that the death probability will then be proportional to the kinetic energy of the avalanche.

For the other parameters (k, a, b and v_1) we have used maximum likelihood estimation subject to the condition that s is continuously differentiable at v_1. This condition gives the equations

$$(8) \qquad b = v_1 - \frac{c - kv_1^2}{2kv_1} \quad \text{and} \quad a = \frac{c - kv_1^2}{v_1 - b}.$$

Direct maximum likelihood estimation together with (8) gives an s curve that is not convincing because it has a very sharp bend at $v \approx 27$ m/s. For this curve $v_1 = 26.7$ m/s. By decreasing the v_1-value the sharpness of the bend is reduced. The s curve shown in Figure 13, which is the one we have used, is obtained by setting $v_1 = 23$ m/s and then maximising the likelihood function subject to (8). To check that the reduction in the v_1-value is not unduly large we have computed the likelihood ratio L(26.7)/L(23) which is 1.75. To be able to reject the value $v_1 = 23$ using a likelihood ratio test at the 10% level would require this ratio to be higher than 3.87 (obtained from the χ^2 distribution with 1 degree of freedom).

Along with the survival probability we work with the death probability, which is defined by

$$(9) \qquad d(v) = 1 - s(v).$$

The estimates obtained for *s* and *d* are of course only valid if the houses in the area where the method is being applied are of similar strength as the houses hit in Súðavík and Flateyri. We believe that this is the case for most of the houses in the avalanche hazard towns in Iceland.

6 AVALANCHE FREQUENCY

In addition to the runout index distribution and survival rate, the third basic ingredient in risk estimation is the frequency of avalanches from the hillside under consideration. The number of avalanches per year is used as a unit for frequency. Note that this is simply the inverse of the return period. Contrary to the first two ingredients, which are estimated globally and once and for all, the frequency estimate is based on the local history of avalanches. As mentioned in the introduction, the frequency estimate is based on a specific runout index that we denote with R. The frequency at a general index r is subsequently related to this reference frequency via the runout index distribution, in accordance with the central assumption also stated in the introduction. While the appropriate choice of R may vary between slopes it is for computational purposes of our method convenient to interpret the frequency estimates in terms of one specific index. The obvious choice is the base index R_0 (= 13), but it would not in fact affect the final risk estimate to make some other choice. The frequency at a general runout index r will be denoted by F_r and we shall refer to F_{13} as the *base frequency*.

6.1 Single path frequency estimation

In Section 4.3 we described how a local estimate of the recording proportion at each runout distance (and hence runout index) was obtained for the 7 main gullies in Neskaupstaður. Before dealing with the case when such a local estimate is available, we will examine the simple case that all avalanches exceeding a runout index $R \geq R_0$ are recorded, but little is known about the recording proportion of shorter avalanches. If N_R avalanches have reached R in a period of T years, and N_R is not too small (e.g. $N_R \geq 4$), then a reasonable estimate of the base frequency is given by

$$F_{13} = \frac{N_R}{T} \cdot \frac{1}{E(R)}$$

where E is the exceedance probability (3). For a simple example, assume that 4 avalanches have reached $r = 15$ in 200 years. Then from Table 5,

$$F_{13} = \frac{4}{200} \cdot \frac{1}{19.4\%} \approx 0.10$$

so that approximately 10 avalanches will reach the base index every century. This method of estimating frequency becomes unreliable if few (one or two) avalanches have reached index R in the period for which it is held that the number of missing avalanches beyond R is negligible, and breaks down completely if no avalanches have reached index R.

Assume now that the local recording proportion q has been estimated and that N_R avalanches exceeding a runout index R have been recorded over a period of T years. Then an estimate of the overall proportion of avalanches exceeding R that have been recorded will be

(10) $$Q_R = \frac{1}{E(R)} \int_R^\infty f(r)q(r)dr$$

where q is the local recording proportion. Thus the frequency at index R is $E(R) \cdot F_{13}$ and one would expect $T \cdot Q_R E(R) \cdot F_{13}$ recorded avalanches exceeding R in a period of T years. The estimate of the base frequency will therefore be

(11)
$$F_{13} = \frac{N_R}{T} \cdot C_R$$

where

(12)
$$C_R = \frac{1}{Q_R E(R)}$$

(which is equal to $F_{13}^{\text{all}} / F_R^{\text{recorded}}$). From F_{13} we may subsequently calculate the frequency at a general runout index r as

(13)
$$F_r = F_{13} \cdot E(r).$$

Note that it follows from (11) and (13) that F_r does in fact only depend on N_R, T, Q_R, $E(R)$ and $E(r)$, i.e. not on the choice of the base index $R_0 = 13$ for the base frequency.

A simple estimate of $q(r)$ is the global recording proportion $p(r)$. Using this amounts to saying that the the recording proportion function is the same in the particular hillside as in the entire 196 avalanche data set. In cases where avalanche records are neither particularly complete nor sparse this should give reasonable accuracy. If $q \equiv p$ (i.e. $q(r) = p(r)$ for all r) and we use the estimate of Section 4.4 for $p(r)$, we may facilitate frequency estimation by calculating the values of C_R for a range of R-values once and for all. We use the notation C_R^* and Q_R^* for the values of C_R and Q_R under this assumption on q and p. Table 8 shows the result of using numerical integration for the calculation of C_R^* and Q_R^*.

R	Q_R^*	C_R^*
13.0	0.201	4.98
13.5	0.243	5.91
14.0	0.298	7.19
14.5	0.365	8.96
15.0	0.445	11.57
15.5	0.538	15.81
16.0	0.640	23.35
16.5	0.743	37.81
17.0	0.836	67.31
17.5	0.908	127.67
18.0	0.953	238.36

Table 8. *Values of C_R^* and Q_R^* used for frequency estimation with $q \equiv p$.*

An important question to ask is how inaccuracy in p and q will affect the final frequency estimate F_r. As before we are estimating the frequency at r from a count of the avalanches that have reached R. From (2), (10), (11) and (13) we obtain

$$F_r = \frac{N_R}{T} \int_r^\infty f_D(t) \frac{1}{p(t)} dt \bigg/ \int_R^\infty f_D(t) \frac{q(t)}{p(t)} dt.$$

We see that F_r is completely independent of $f_D(t)$, $p(t)$ and $q(t)$ for $t < \min(r, R)$. If $r > R$ it is apart from $f_D(t)$ sufficient to have an estimate of the ratio $q(t)/p(t)$ in the interval $[R, r]$. It is

only for $t > r$ that we need separate estimates of $p(t)$ and $q(t)$. This is in particular noteworthy in the case when we choose to set $q \equiv p$. If this is in fact valid for $t > R$, then the final risk estimate will be independent of any errors in $p(t)$ for $t < r$. In the case $r < R$ we see that F_r is independent of the values of $q(t)$ in the interval $[r, R]$. For $t > R$ we again need separate estimates of p and q.

Note that there is a trade-off in the choice of R. In order to make the frequency estimate as reliable as possible, one would like to make N_R as large as possible, and thus choose R as small as possible. But one would also like to reduce the length of the r-interval where one may have unreliable estimates of p and/or q and thus choose R as large as possible. This suggests that R should be chosen low enough that a few avalanches have exceeded R but not much lower.

The reliability of the frequency estimate can also be enhanced by choosing more than one value for R. In practice we have often chosen $R = 13, 14, 15$ and 16, and then taken the average of the resulting frequency estimates (perhaps suitably weighted).

For a simple example, assume that we are setting $q \equiv p$ and that 6 avalanches have been recorded that exceed $r = 14.5$ in 90 years. Then from Table 8,

$$F_{13} = \frac{6}{90} 8.96 \approx 0.60$$

i.e. six avalanches a decade exceeding $r = 13$ would be expected on average. But we also see from the table that $Q_{13}^{*} \approx 1/5$, saying that during the last century about one fifth of all avalanches in the paths of the data set with $r > 13$ have been recorded, if the assumptions are correct. The average frequency of recorded avalanches exceeding $r = 13$ should therefore be $0.6/5 = 0.12$, i.e. about 11 such avalanches should have been recorded over the 90 years. Finally, let us see what the comments after Table 8 tell us in this example. If the intention is to estimate the risk at, say, $r = 16$ then we only need frequency estimates for $r > 16$ and these will in fact only depend on the values of $q(r)/p(r)$ in the interval $[14.5, 16]$ and the values of $p(r)$ and $q(r)$ for $r > 14.5$, as well as the values of $f_D(r)$ for $r > 14.5$.

6.2 Several gullies

If avalanches fall mostly from isolated gullies deemed to have the same topography, then the frequency can be jointly determined for all gullies, in order to increase the accuracy. If there are M gullies and N_R, T and C_R are as in Section 6.1 (N_R is the total number of avalanches reaching R from all the gullies) then the base frequency in each gully is estimated by

(14)
$$F_{13} = \frac{N_R}{MT} \cdot C_R.$$

We are on slippery ground here, because if the gullies have different recorded frequencies and the reason is in fact that they are differently shaped (or collect snow differently), then we might be worse off than by estimating the frequency in each gully individually. To aid in this decision, one can apply some statistical test to see if one can reject the null hypothesis, that all the gullies are the same, against the alternative that they are different. This approach might even be extended to the case when there is not reason to believe that the frequencies are equal, but one is prepared to make a subjective guess on the relative frequency of each gully.

Let us now look more closely at the example from Neskaupstaður already mentioned in Sections 4.3 and 4.4. Table 9 lists all the recorded avalanches with runout index 12 or higher from 7 big gullies above the town.

The average maximum width of the avalanches with recorded width is 170 m but if we just take the avalanches that reach runout index 14 we obtain an average maximum width of 244 m. We return to the question of width in the next section.

Let us emphasise that the purpose of this example is to demonstrate the use of the method, and while we shall assume that the avalanche frequency of each gully is the same, we do not necessarily believe this to be the case in reality. Now set the observation period to 110 years (there is a recorded avalanche in 1885 in Neskaupstaður that does not qualify for entry in Table 9). The recording proportion distribution, q, was estimated as explained in Section 4.4 with the result of Figure 6.

From Table 9, Table 5, (10) and (14) with $M = 7$ we then obtain the 3 different estimates of F_{13} shown in Table 10. Note that in this case $p \not\equiv q$ so we cannot use Table 8 to obtain Q_R and C_R but must instead re-evaluate them. Note also that we give F_{13} in percentages, so the values can be interpreted either as the probability that in 1 year an avalanche from a particular gully reaches index 13, or as the number of avalanches per century that reach 13. We infer from the table that the base frequency is about 5 avalanches per century.

Gully	Data base no.	Date	Runout index	Maximum width (m)	Into sea
Bræðslugjár	135	Jan./Feb. 1936	15.4	130	
	136	04.11.1981	12.1	?	
	138	04.02.1974	12.9	220	
	139	20.12.1974	15.6	415	x
	142	04.02.1974	12.8	100	
Miðstrandarskarð/Klofagil	145	Jan. 1936	14.2	130	
	146	20.12.1974	14.8	270	x
	N/A	21.03.1989	13.3	60	
Ytra and Innra Tröllagil	149	Jan. 1894	15.1	?	x
	150	March 1920	13.6	140	
	154	04.02.1974	12.4	?	
	155	27.12.1974	13.5	190	
Urðarbotnar/Sniðgil	156	27.-28.12.1974	13.6	60	
	157	04.02.1974	12.2	?	
	158	28.12.1974	13.1	60	
Drangaskarð/Skágil	160	24.01.1894	15.4	390	
	161	04.02.1974	13.5	220	
	162	20.12.1974	14.4	390	
	163	20.-21.12.1974	12.4	40	
Nesgil	167	Feb. 1966	14.7	120	
	168	04.02.1974	13.2	90	
	169	19.12.1974	15.2	180	
	220	21.03.1989	13.6	130	
Bakkagil	170	Feb. 1966	14.3	150	
	171	04.02.1974	13.7	70	
	172	20.12.1974	16.4	260	
	221	21.03.1989	13.6	100	

Table 9. *Long recorded avalanches from 7 gullies in Neskaupstaður.*

R	N_R	$E(R)$	Q_R	C_R	F_{13}
13.0	20	100%	49%	2.0	5.3%
14.0	11	47%	66%	3.2	4.6%
15.0	6	19%	79%	6.5	5.1%
16.0	1	7%	86%	17.3	2.3%

Table 10. *The number of avalanches reaching different runout indices in Neskaupstaður and corresponding estimates of the frequency of 13-avalanches from each gully.*

6.3 Frequency in hillsides

If we are considering a straight hillside where it is deemed that avalanches fall from each part with equal probability a slightly different approach is required. Assume the total width of the hillside is W and the estimated avalanche width is A. If N_r, T and E are as before the resulting estimate of the base frequency is given by

(15)
$$F_{13} = \frac{A}{W} \cdot \frac{N_R}{T} \cdot C_R.$$

If for instance the area is 800 m wide, an avalanche is 400 m wide, the estimate of Q_{13} is ¼, and 5 avalanches are recorded with runout index greater than 13 in 50 years of observation, then from (12) we obtain $C_{13} = 1/(Q_{13}E(13)) = 1/(¼ \cdot 1) = 4$ and from (15) the frequency estimate at 13:

$$F_{13} = \frac{400}{800} \cdot \frac{5}{50} \cdot 4 = 0.2 \text{ per year.}$$

Notice that A is the *average* avalanche width or more precisely the width of an *equivalent* rectangular avalanche where the meaning of *equivalent* is admittedly somewhat vague. In fact we have in practice been working with the more easily determined *maximum* avalanche width instead of the *average* width. This causes overestimation of the risk and to compensate we pull the calculated risk lines towards the mountain. We explain this in more detail in Section 7.3.

We point out that we have assumed here that the width of an avalanche is independent of its runout distance. This is of course not true in reality, as long avalanches tend to be wider. In practice we have dealt with this problem case by case in a rudimentary fashion, but the relationship between avalanche runout and avalanche width would of course deserve a study. Keylock (1996) has considered how avalanche width depends on avalanche size on one hand, and how avalanche runout ratio depends on avalanche size on the other.

7 RISK MODEL

7.1 Speed profiles

In Chapter 5 we used the PCM model to estimate the speed of an avalanche at a given point in its path. A graph showing such estimated speed of an avalanche at each runout index along its path will be called the *speed profile* of the avalanche. Examples of speed profiles of avalanches from Skollahvilft are given in Figure 14. Each line in the figure shows the speed profile of the avalanche with the runout index shown at the start of the line (on the left side of the graph). The speed profile is determined by simulating the avalanche with the PCM model using the (M/D, μ) pair on the parameter axis of Section 3.3 that will explain the avalanche.

We will denote by $v_r(t)$ the speed at r of the avalanche that stops at t. Thus each of the lines in Figure 14 is a graph of v as a function of r for a particular t. The uppermost line shows for instance the graph of $v_r(20)$, the speed of the avalanche stopping at runout index 20, as calculated by the PCM model with the parameters $(M/D, \mu) = (863 \text{ m}, 0.082)$. The reason for our notation is that in the risk formula in the next section we will consider $v_r(t)$ as a function of t. To make it easier to visualise this we show the graphs of v_{15} and v_{18} in Figure 15, and show by filled and open circles corresponding points in the two figures.

Finally we note that researchers have observed that, for parameter pairs in the same range as we have been using, the PCM model tends to underestimate the real speed (see e.g. McClung 1990), and that this holds true more generally for so-called Vollemy-fluid models (Bartelt and Salm 1998). While it would of course be desirable to use a model that resulted in better speed estimates, this effect is counteracted by the fact that the empirical survival function, that we obtained in Chapter 5, and also enters into the risk formula below, is obtained using the same PCM model.
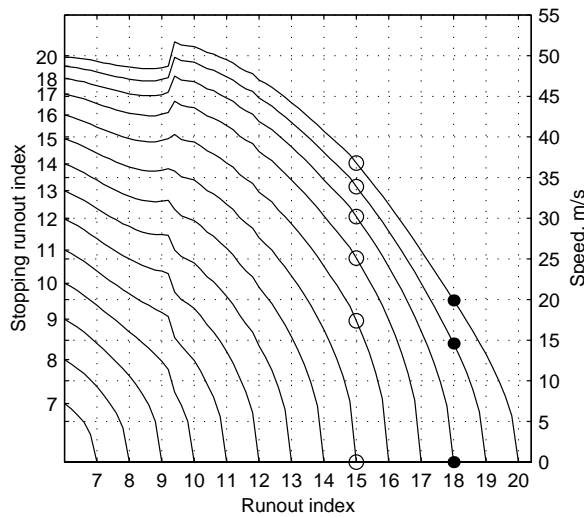

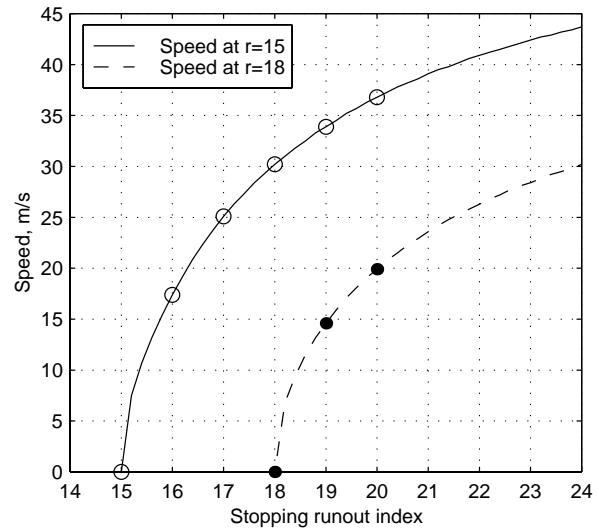Figure 14. *Speed profiles from Skollahvilft according to runout index.*

Figure 15. *Speed at two places under Skollahvilft according to stopping runout index.*

7.2 Formulae for risk

We now have all the necessary ingredients to present the formula for calculating the risk of living or working in a building under an avalanche hillside. The total risk will be the aggregate of the risk from short, medium and long avalanches. Depending on the placement of the building the different length avalanches will contribute differently to the total risk. The long avalanches will be rare, but devastating when they fall. The short avalanches are more frequent but not as harmful (or even totally harmless if the building is not within their reach).

Assume that the building is placed at runout index r and let the base frequency be F_{13} (frequency of avalanches that reach runout index 13). By (13) the frequency of avalanches past the building is $F_r = F_{13} \cdot E(r)$. The risk formula is most accurately presented as an integral but this is (maybe) not very transparent so we begin by presenting a rather rough approximation that we hope is more evident. Denote with v the speed of the avalanche in m/s when going past the building, and let $P(A)$ be the probability that event A occurs in a one year period. Let

$d(v)$ be the death probability given by (7) and (9). If no avalanche can hit the building with a speed greater than 50 m/s we obtain the following approximate formula for the risk of a person that spends all his time in the building:

(16)   Risk = $P(0 < v \le 10) \cdot d(5) + P(10 < v \le 20) \cdot d(15) + \ldots + P(40 < v \le 50) \cdot d(45)$.

We can calculate the probabilities $P(v_1 < v \le v_2)$ using a table of speeds and runout indices calculated with the PCM model. The more accurate integral formula is

(17) $$\text{Risk at } r = F_{13} \int_r^\infty f(t) d(v_r(t)) dt$$

where f is the runout index density function. This is the formula that we have actually been using, together with numerical integration. The result is however modified due to a so-called tongue effect that we explain in the next section.

7.3 Tongue effect

It is quite possible that a house is missed by an avalanche that goes further than the house, due to the effect demonstrated in Figure 16 where a house at runout index 17 is missed by an avalanche of runout index 18. We are well aware of the effect but so far we have dealt with it in a rather rudimentary fashion.
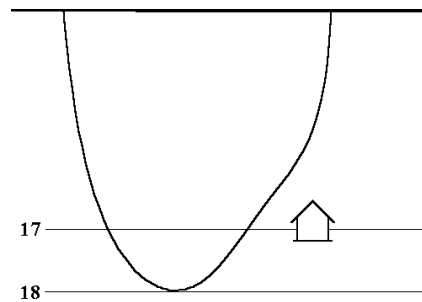

Figure 16. *The tongue effect.*

We selected a small set of about 7 avalanches with different tongue shapes that were deemed to be representative for the shapes of all the avalanches in the collection. We then calculated the position of several risk lines under the standard path using the risk model described above, assuming that the runout distance was distributed according to the global runout index distribution of Section 4.4 and that the shapes were selected at random from the 7. We then repeated the calculation under the assumption that all the avalanches were rectangular and it turned out that equivalent risk lines were further away from the mountain by about 60 m, corresponding to 6/10 of a runout index. The calculation was done using a few different frequencies and we also checked the result in a few other paths. The results differed a bit, but remained in the neighbourhood of 0.6 runout indices.

Under straight (gully-less) hillsides the tongue effect can therefore be taken into account by pulling all calculated risk lines towards the mountain by a distance corresponding to 0.6 runout indices.

A more satisfactory approach might be to divide each avalanche in the underlying data set into a fixed number (5 say) of segments of equal width thus allowing the recording of runout distances of different tongues rather than simply the longest one. In the estimation of the

runout index distribution we would subsequently treat each segment as a single avalanche. No further modification of the result of the risk formula would then be required.

Under gullies the situation is a bit more complex since a house that is a little to the side of the main direction from the gully can escape both because of the shape of the avalanche and because the avalanche takes a direction away from the house when leaving the mouth of the gully. On the other hand it is possible that the risk lines should be pulled less back directly under the gully because the tip of a gully avalanche is often there. Up till now we have been solving this problem quite heuristically, case by case, but of course further investigation of the tongue effect under gullies is desirable (see Section 7.6).

7.4 Effect of changing the parameter axis

The choice of the parameter axis in Section 3.3, which has been used throughout this report, was somewhat subjective. Thus it is important to note that this choice will affect all the different ingredients of the final risk formula (17), the shape of the density function, f, the speed estimate, v, the empirical relationship between death rate and speed, d, and the frequency estimate, F_{13}. While we have argued that the estimated risk should not be too sensitive to change in axis, we have made some investigations into the effect of such change, in an attempt to quantify this claim. In this section we report shortly on the major findings of these investigations.

For the comparison we have considered two alternative parameter axes, one that lies to the left of the main parameter axis, and one that lies to the right of it. All three parameter axes are shown in Figure 17. For ease of reference the figure also shows a selection of isorunlines and the positions of runout indices. The right axis has been chosen to pass through the minimum of the mean square deviation of Figure 3 (marked with * here), and the left axis is one that we used in some earlier implementations of our approach. The equation of the main axis is given by (1), that of the left axis is $\mu = 0.513 - 0.000797 \cdot M/D$, and that of the right axis is $\mu = 0.825 - 0.0003\ M/D$.
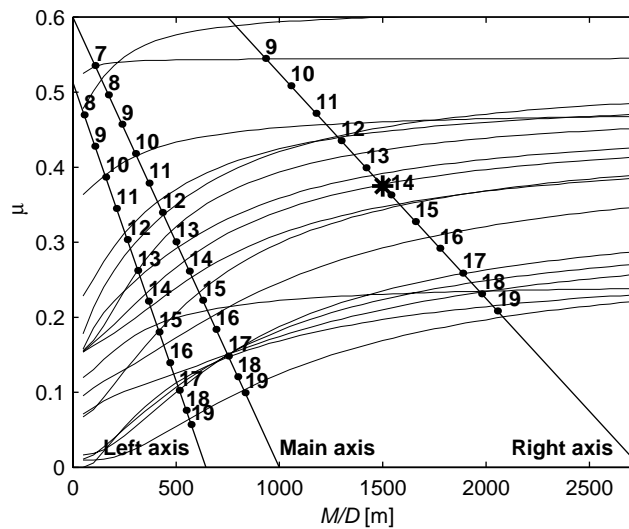

Figure 17. *Three parameter axes and isorunlines for every 20th avalanche as well as the shortest and the 4 longest according to the scale of each parameter axis. The numbers along the axes are runout indices.*

The risk comparison involves the estimation of the risk at two horizontal distances, x_{13} and x_{16}, in each of the 81 paths of the data set using each of the three parameter axes. The points are chosen where the main axis runout index is 13 and where it is 16.

For each of the two alternative parameter axes we have repeated the estimation of the runout index data density, f_D. We then determined, for each of the 81 paths, the recording proportion at each point on the path, according to the main axis runout index of the point, using the function p of Section 4.4. To find the appropriate recording proportion function for the new axis we have, for each (new) runout index, located the corresponding point on each of the 81 paths, and then taken the average of the recording proportions at these points. The real density function f was then determined using (2). To determine the avalanche speed that enters into the risk formula (17) we selected appropriate pairs on the new axis and simulated again with the PCM model. It was also important to repeat the survival probability estimation of Chapter 5 in order to obtain a revised d, because the PCM model gives consistently higher speeds when the axis is moved to the right in the $(M/D, \mu)$ plane.

Having obtained the new f, v, and d that enter into the risk formula (17), the only remaining quantity is the base frequency, F_{13}. For this, we set the frequency to 1 at x_{13}, and then use (13) to determine F_{13} (the frequency where the new runout index is 13). In this way we are factoring out the frequency estimation, in effect assuming that the frequency has been determined at x_{13} and observing the effect on the risk estimate of changing the axis.

The results of the comparison are given in Figure 18 and Table 11. As an example of how to read the histograms, there are 25 hills where the risk estimate at x_{16} is between 30% and 40% lower for the left axis than for the main axis. In addition to the average risk change, Table 11 also gives the average change in the estimated frequency, at x_{16} and x_{18} (where the (main axis) abstract runout index is 18). The relatively large increase in the frequency when moving to the right axis indicates that the runout index distribution corresponding to the right axis has a thicker tail than the main one.

Axis line used	Average risk change		Average frequency change		
	x_{13}	x_{16}	x_{13}	x_{16}	x_{18}
left	-4.9%	-16.4%	0.0%	-8.5%	-5.4%
right	0.4%	74.7%	0.0%	45.8%	75.4%

Table 11. *Average change in estimated risk and frequency when moving from parameter axis of Section 3.3 to two other parameter axes.*

A credible explanation of the risk increase at x_{16} when moving to the right axis, is that the longest avalanches have a longer runout on average after transfer to the other hills using the right axis, than when the main axis is used. One difficulty with checking this claim is that the set of 'longest avalanches' is not well defined, as it depends on which axis is used. However, if the 5 longest avalanches according to each axis are chosen then a set of 7 avalanches is obtained. If these avalanches are transferred to each of the 81 hills using the right axis their transferred runout is 60 m longer on average than when the main axis is used. If the 10 longest are chosen for each axis a set of 16 is obtained and their transferred runout is on average 40 m longer when the right axis is used. This may be compared with the average distance one must move uphill from x_{16} to increase the risk by 75%, which we have calculated to be 39.8 m, using the 81 hills and (17) with the main axis.
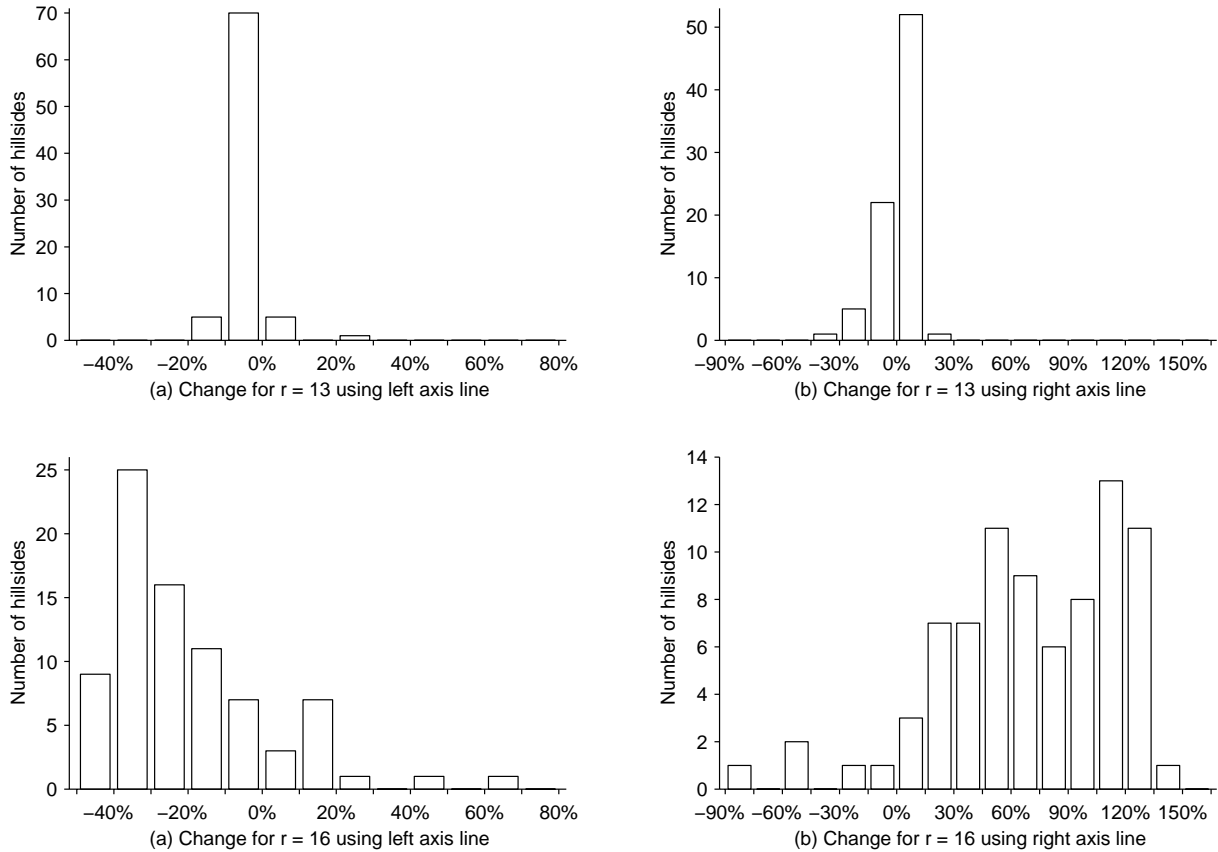
Figure 18. *Summary of the change in estimated risk at r = 13 and r = 16 for all 81 paths of the Icelandic data set when moving from the parameter axis of Section 3.3 to lines that lie (a) further to the left and (b) further to the right.*

To further investigate the changes in risk we tried changing only the speed and survival probability in (17), leaving $f(t)$ unchanged. When moving to the left axis the average risk change turned out to be – 4.5% at $r = 13$ and –10.2% at $r = 16$, thus accounting for most of the risk change. When moving to the right axis, however, the average effect on the risk was negligible, 0.0% at $r = 13$ and 0.8% at $r = 16$.

In our opinion these results support our claim that the risk estimate is not unduly sensitive to changes in the parameter axis. It may be further kept in mind that in accordance with the discussion in Section 3.2 the runout index distribution may be viewed as a one-dimensional projection of the "true" two-dimensional parameter distribution and from this viewpoint some weighted average of estimates based on different axes might be used. In a similar vein it is of some value to estimate the risk in a particular hillside using several parameter axes. If they all give similar results, the confidence in the results is increased, and vice versa if the outcomes differ widely.

7.5 Acceptable return period

The frequency estimates that we have obtained working with the method vary considerably, ranging from less than 1 avalanche per century reaching $r = 13$ to values approaching 1 avalanche per year reaching $r = 13$ (cf. the estimate $F_{13} = 0.75$ obtained for Skollahvilft just after Table 4, the estimate $F_{13} = 0.1$ of Section 7.6 for Súðavík and the estimate $F_{13} = 0.05$ of Section 6.2 for Neskaupstaður). In Table 12 the relationship between risk, frequency and return

period is considered. The table is calculated using the main parameter axis and the standard path, but the results are neither very sensitive to the chosen path nor the axis. It is quite noteworthy that we find that to reach an acceptable risk level a much higher return period than previously reckoned is necessary — 3000 to 8000 years depending on frequency, compared with 300 years in Swiss regulations and 1000 years in Norwegian regulations (Salm et al. 1990; Lied 1993, but see the discussion in Section 2.4). The increase in return period with decreasing base frequency is caused by the fact that the exceedance probability, E, dies out very quickly for r higher than about 18. If $E(r)/E(r + 1)$ were constant then the risk-return period relationship would be independent of frequency, but it is easy to see from Table 5 that our estimate of E decreases much faster than this.

	Return period, years		
Base frequency	Risk = 3×10^{-4}	Risk = 1×10^{-4}	Risk = 0.3×10^{-4}
Low, $F_{13} = 0.01$	1000 (r=15.1)	2600 (r=15.8)	7700 (r=16.6)
Medium, $F_{13} = 0.1$	700 (r=16.6)	2100 (r=17.3)	5100 (r=18.1)
High, $F_{13} = 1$	500 (r=18.1)	1100 (r=18.6)	2900 (r=19.1)

Table 12. *Return period according to base frequency and risk. The numbers are obtained using the standard path.*

The values for the risk chosen in Table 12 correspond to the boundaries between differently coloured zones according to the Icelandic draft regulations for avalanche hazard mapping. These state that areas where estimated risk is greater than $3\cdot10^{-4}$ should be coloured red, those where the risk is between $1\cdot10^{-4}$ and $3\cdot10^{-4}$ should be blue, yellow between $0.3\cdot10^{-4}$ and $1\cdot10^{-4}$, and "safe" areas should be white. Recall that $0.3\cdot10^{-4}$ is the acceptable risk level for living houses, discussed in Section 2.3.

7.6 Examples of risk calculation

In this section we shall consider two examples of risk estimation, one under Bakkagil in Neskaupstaður (one of the 7 gullies discussed earlier), and the other under the hill in Súðavík. Let us emphasise that the results should not be viewed as final risk estimates for these areas, but rather as examples of the use of the methodology presented herein.

Let us look first at Bakkagil. We have already estimated the base frequency for each of the 7 gullies as $F_{13} = 5$ avalanches per century (see the end of Section 6.2). Using this value together with (17) we have calculated the positions of the three risk levels of the draft regulations discussed in the last section.

As mentioned at the end of Section 7.3 some heuristic must be used to take the tongue effect into account under a gully. We have taken the course of pulling the calculated position 0.3 runout indices uphill on the centre line (directly under the gully), and 1.2 runout indices uphill at reference points 200 m on either side of the centre line. The risk line is then obtained by drawing a smooth parabola like curve through these three points. If the risk line really is a parabola, then this corresponds to an average pulling of 0.6 runout indices over a 400 m wide area under the gully, in accordance with the recommended value of Section 7.3. The distance of the reference points on either side from the centre line (200 m), corresponds to an average width avalanche of 300 m that is allowed to sway 50 m to either side on leaving the gully mouth.

The resulting risk lines are shown on the map in Figure 19 (dashed lines), together with runout indices (unbroken lines), and the reference points (filled circles). By (13) the return

period is approximately 5700 years at the 0.3 risk line, 2100 years at the 1.0 risk line and 800 years at the 3.0 risk line. Moreover, the map shows the location of the Bakkagil profile (Nesk25aa), and outlines of recorded avalanches from Bakkagil (unbroken) and the neighbouring gullies (dashed). Two adjacent profiles, not shown on the map, were also used for the calculation. Note that the map only shows risk due to avalanches from Bakkagil. A final risk map would have to add the risk due to avalanches from the nearby gullies.
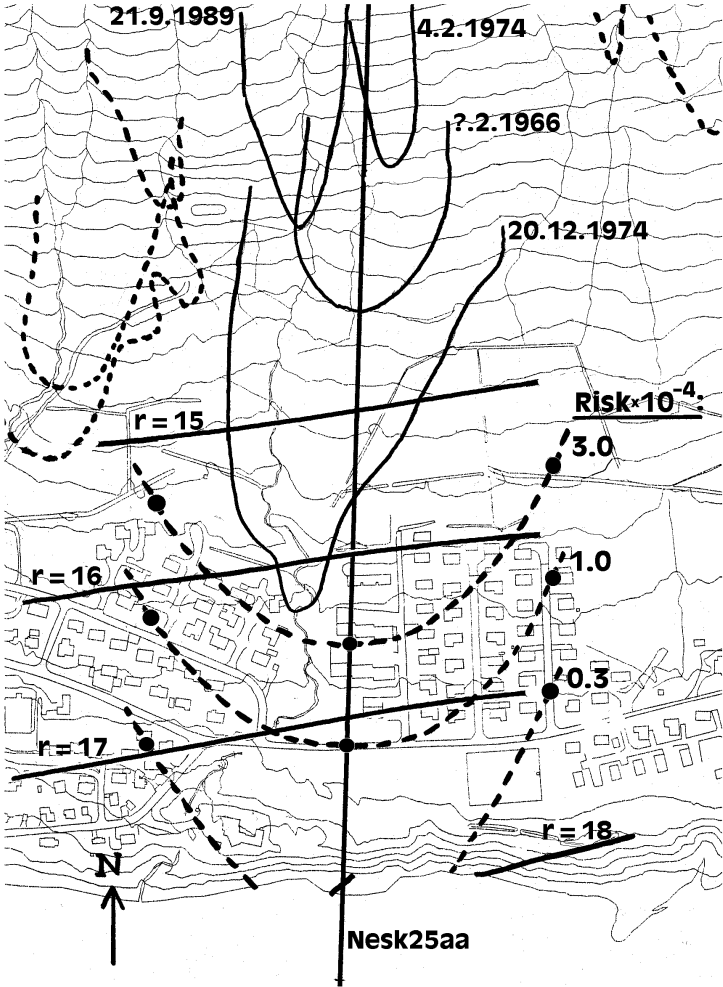

Figure 19. *Risk estimation due to avalanches from Bakkagil, Neskaupstaður. Scale 1:7500. See main text for explanations.*

It is of interest view the function under the integral in (17) to see the contribution of avalanches with different runout indices to the total risk. In Figure 20 this function is shown for a house at $r = 16$. The 5%, 25%, 75% and 95% percentile points are at runout indices 16.3, 16.7, 17.8 and 19.1 respectively, so that 90% of the risk is caused by avalanches going between 0.3 and 3.1 runout indices beyond the house and half the risk is caused by avalanches going between 0.7 and 1.8 indices beyond it. Similar graphs are obtained in other paths and for other values of r, except that the distribution is narrower for higher r-values.
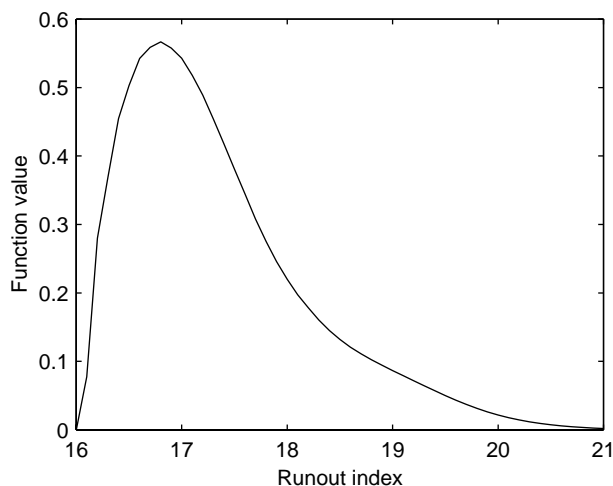
Figure 20. *The distribution of risk with runout distance for a house at r = 16 in Bakkagil. The graph shows the function under the integral in (17), normalised as a density function.*

Now turn the attention to Súðavíkurhlíð, the hillside above Súðavík. Here we have yet to estimate the base frequency. We regard Súðavíkurhlíð to be a 'straight hillside' and use Section 6.3. The total width of the area considered is $A = 750$ m and there are four recorded avalanches exceeding runout index 13. Details of these are given in Table 13.

Database no.	Profile	Date	Runout index	Width
24	Suhl01aa	06.01.1983	14.5	175 m
25	Suhl02aa	06.01.1983	15	100 m
30	Suhl02aa	18.12.1994	14.3	40 m
31	Suhl04aa	16.01.1995	16.1	275 m

Table 13. *Recorded avalanches from Súðavíkurhlíð.*

The average width of these avalanches is 148 m. However, long avalanches tend to be wide, and we choose to use an avalanche width of $W = 200$ m, based on that fact and experience from elsewhere. Based on the ages of the houses in the village we judge the observation period to be $T = 60$ years. We have also chosen to use $q \equiv p$ and thus we may use the values of C_R^* from Table 8. We may now use (15) to estimate the base frequency, and as earlier we choose to use several values of R. Table 14 gives the details of the calculation.

The average of the obtained F_{13} values is 10.0%. Now (17) may be used to calculate the risk at selected points in the village, and this time we may use constant tongue effect pulling of 0.6 runout indices everywhere. The result is shown on the map in Figure 21. On the $20 \cdot 10^{-4}$ risk line the runout index is 15.4 and the return period calculated with (13) is 150 years, and on the $50 \cdot 10^{-4}$ risk line the runout index is 14.7 and the return period 70 years. If the risk is $50 \cdot 10^{-4}$, the exposure is 60%, and one lives in the house for 40 years, then the probability of being killed in an avalanche is about 12%!

40

R	A/W	T	N_R	C^*_R	F_{13}
13	0.267	60	4	4.98	8.9%
14	0.267	60	4	7.19	12.8%
15	0.267	60	1½	11.57	7.7%
16	0.267	60	1	23.35	10.4%

Table 14. *Base frequency calculation in Súðavíkurhlíð.*
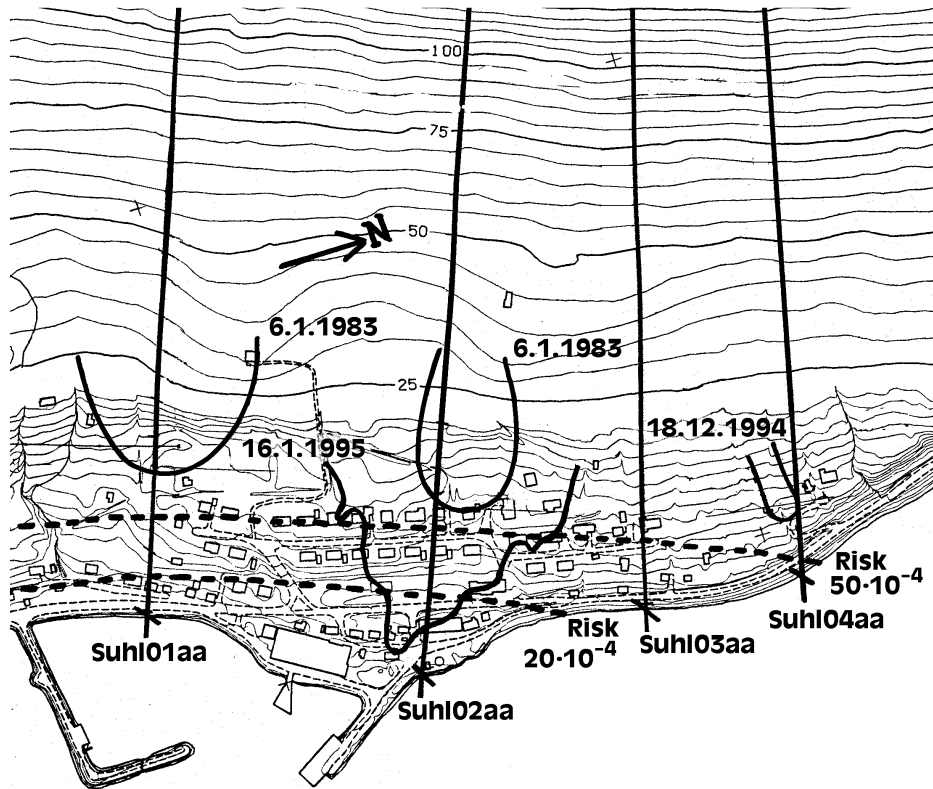

Figure 21. *Avalanche risk in Súðavík. Scale 1:7500. See main text for explanations.*

8   CONCLUDING REMARKS

The method described herein is designed for assessing the risk caused by avalanches from hillsides that have some recorded history of avalanches. We have not described a comprehensive method for avalanche hazard zoning that takes everything into account. It will not help in identifying starting zones of avalanches. It is not suitable for assessing the risk from slush flows or mud flows. The method is not really suited for hillsides where there is no avalanche history, although it can be used to put an upper limit on the risk under such hillsides, and it is not suitable in its present state for hazard evaluation of areas that are protected by defence walls or supporting structures.

We remind the reader of some of the shortcomings and possible improvements that we have mentioned along the way. Among them are the need to improve the handling of the tongue effect, a study of the tongue effect under gullies, the study of the relationship between avalanche width and runout distance, the dependence of survival on the size of an avalanche as well as its speed, and a better estimate of the global runout index distribution using the age of houses. To tailor the method for low hills a study of fatalities due to smaller avalanches would

be necessary, as well as a study of their runout distances. One would also like to try using the method with more sophisticated physical models that hopefully describe real avalanches better than the PCM model. Another idea is to use a combination of topographical models and physical ones. For the topographical model we have in particular in mind a method suggested by Guðmundsson (1996), which, in contrast with methods based on alpha-beta models or runout ratios, uses information on the full profile of each avalanche path and then generates for a given path the analogue of the data density function. Along with such improvements it is important to consider how one should possibly restrict or subdivide the data set in a clearly defined manner, in order to ensure that the underlying assumption behind our approach, stated in the introduction, holds true. Most likely, however, a balance has to be drawn between satisfying this assumption and not making any subset of avalanches unduly small.

Finally we wish to describe an important approach to checking the validity of the proposed risk estimates. For each house, both present and past, in the Icelandic towns under avalanche risk, use the method to calculate the risk. For each house, determine the length of time that it has been standing, and estimate the expected average number of people present in the house during each period of its existence. The risk may then be integrated to find the expected total number of people that would have been killed in the last 120 years (about the age of the towns) based on the risk being as calculated. This number may then be compared with the actual number of fatalities. Indeed, a central advantage of the approach outlined in this report is that it lends itself to quantitative checks of this kind.

REFERENCES

Bakkehøi, S., U. Domaas and K. Lied 1983. Calculation of snow avalanche runout distance. *Ann. Glaciol.* 4, 24–29.

Bartelt, P. and B. Salm 1998. A short comparison between Vollemy fluid and Criminale-Ericksen-Filby-fluid dense snow avalanche models. In: E. Hestnes (editor), 25 years of snow avalanche research, Voss, May 12-16, 1998. *Norwegian Geotechnical Institute Publications* 203, 65–69.

Chapman, C.R. and D. Morrison 1994. Impacts on the Earth by asteroids and comets: assessing the hazard. *Nature* 367, 33–40.

Evans, A.W., P.B. Foot, S.M. Mason, I.G. Parker and K. Slater 1997. Third party risk near airports and public safety zone policy. *R&DD Report* 9636. National Air Traffic Services Ltd, London.

Grímsdóttir, H. 1998. Byggingarár húsa í Neskaupstað (building years of houses in Neskaupstaður). *Greinargerð Veðurstofu Íslands.* Report VÍ-G98011-ÚR09. Reykjavík, 35 pp.

Guðmundsson, G. 1996. A topographical model for avalanches. Talk presented at work meeting on snow avalanches at the Icelandic Meteorological Office, January 11-12, 1996. Unpublished.

Jóhannesson, T. 1998a. Return period for avalanches on Flateyri. *Greinargerð Veðurstofu Íslands*. Report VÍ-G98008-ÚR07. Reykjavík, 12 pp.

Jóhannesson, T. 1998b. Icelandic avalanche runout models compared with topographical models used in other countries. In: E. Hestnes (editor), 25 years of snow avalanche research, Voss, May 12-16, 1998. *Norwegian Geotechnical Institute Publications* 203, 43–52.

Jónasson, K. and Þ. Arnalds 1997. A method for avalanche risk assessment. Short description. *Greinargerð Veðurstofu Íslands.* Report VÍ-G97036-ÚR28. Reykjavík, 16 pp.

Keylock, C.J. 1996. *Avalanche risk in Iceland*. M.Sc. thesis, Department of Geography, Faculty of Graduate Studies, University of British Columbia.

Keylock, C.J., D.M. McClung and M.M. Magnússon 1998. *Avalanche risk by simulation*. To appear in *J. Glaciol.*

Lied, K. 1993. Snow avalanche experience through 20 years. *Laurits Bjerres Minneforedrag* 14. Laurits Bjerrums Minnefond, Norwegian Geotechnical Institute, 42 pp.

Lied, K., C. Weiler, S. Bakkehøi and J. Hopf 1995. Calculation methods for avalanche runout distance for the Austrian Alps. *Norwegian Geotechnical Institute Report* 581240-1.

McClung, D.M., A.J. Mears and P. Schaerer 1989. Extreme avalanche runout data from four mountain ranges. *Ann. Glaciol.* 13, 180–184.

McClung, D.M. 1990. A model for scaling avalanche speeds. *J. Glaciol.* 36(123), 107–119.

Perla, R., T.T. Cheng and D.M. McClung 1980. A two-parameter model for snow avalanche motion. *J. Glaciol.* 26(94), 197–207.

Salm, B., A. Burkard and H.U. Gubler 1990. Berechnung von Fliesslavinen. Eine Anleitung für den Praktiker mit Beispielen. *Mitteilungen* 47. Eidgenössisches Institut für Schnee- und Lavinenforschung, Davos.

Sigurðsson, S.Þ., K. Jónasson and Þ. Arnalds 1998. Transferring avalanches between paths. In: E. Hestnes (editor), 25 years of snow avalanche research, Voss, May 12-16, 1998. *Norwegian Geotechnical Institute Publications* 203, 259–263.

Silverman, B.W. 1986. Density estimation for statistics and data analysis. In: D.R. Cox, D.V. Hinkley, N. Reid, D.B. Rubin and B.W. Silverman (general editors), *Monographs on statistics and applied probability* 26. Chapman & Hall, London, 175 pp.

Wilhelm, C. 1997. Wirtschaftlichkeit im Lavinenschutz – Methodik und Erhebungen zur Beurteilung von Schutzmassnahmen mittels quantitativer Risikoanalyse und ökonomischer Bewertung. *Mitteilungen* 54. Eidgenössisches Institut für Schnee- und Lavinenforschung, Davos, 309 pp.